<u>REMARKS</u>

<u>Rejection of claims under 35 U.S.C. 112</u>:

Claim 1 has been rejected under 35 USC 112, first paragraph, for containing new matter. The Office Action states that no literal or figurative support is provided in the specification for "mammalian intracellular physiological conditions." Applicants have amended the claim to cite "mammalian physiological conditions" to obviate the rejection. It is the Applicants' opinion that mammalian physiological conditions are well established in the art.

The specification states on page 3 lines 3-5 and on page 4 lines 5-8 that the intended use of the labile disulfide bond is for delivery to a cell. On page 25 of the specification, in lines 18-21, use of a signal is described for directing a labile disulfide-containing compound or complex to: "a cell location (such as tissue cells) or location in a cell (such as the nucleus, or cytoplasm) either in culture or in a whole organism." The stated purpose of the transduction signal, page 25 lines 29-30, is to transport molecules across membranes and thus into a cell. Lines 2-3 on page 30 state that "biologically active compounds utilized in this specification are designed to change the natural processes <u>associated with a living cell</u>" (underline added).

Utility of the invention is for commercial research of therapeutic methods and for mammalian production of proteins. Support in delivering compounds to cells in a mammal *in vivo* can be found on page 3 lines 17-19 and 30 and on page 29 lines 8-10. In examples 10 (page 38), 15 (page 42) and 48 (page 63), Applicants demonstrate delivery of labile disulfide bond-containing compounds to: HeLa cells, mammalian (human) epithelial cells; HepG2 cells, mammalian (human) liver cells; 3T3 cells, mammalian (mouse) fibroblast cells. Applicants have shown the effectiveness of the compounds *in vivo* in mice (examples 25, 27, 31 etc.) and *in vivo* in rat (example 26).

Claim 13 has been rejected for lack of antecedent basis for the term molecule. Claim 13 has been amended to more clearly indicate the relation of the addition of a nucleic acid to the compound of claim 1 as requested by the Examiner. Support for the amendment can be found on page 4 lines 1-19 and in examples 13, 14, 23-27, 30, 31, 34, 36, 38, 40, 41 and 48.

<u>Rejection of claims under 35 U.S.C. 102</u>:

Claims 1, 5, and 6 have been rejected under 35 USC 102(a) as being anticipated by Bulaj et al., as evidenced by Szajewski et al. and by Keire et al. The Office Action states that Bulaj et al. and Keire et al. teach the attachment of a transduction signal linked to a disulfide-containing compound wherein the disulfide has a lower pKa that glutathione. The Action states that because the peptides taught in Bulaj et al. and Keire et al. are cationic, and because the specification teaches that transduction peptides are cationic, the peptides in Bulaj et al. and Keire et al. therefore meet the structural limitations required by the claims. Applicants respectfully disagree. The statement that transduction peptides are cationic does not require that all cationic peptides be transduction peptides. An analogy can be made to the statement that while all squares are rectangles, not all rectangles are squares. The physical requirement for a transduction signal is the ability to "transport themselves and attached molecules across membranes" (page 25 lines 29-30). Direct evidence that not all cationic peptides act as transduction signals can be found in Wender et al. 2000 (PNAS 97(24): 13003-13008). Wender et al state in the abstract "Charge alone, however, is insufficient for transport as

oligomers of several cationic amino acids (histidine, lysine, and ornithine) are less effective than Tat$_{49-57}$ in cellular transport." See also figures 1 and 2 on page 13005 of Wender et al.

It is Applicants' opinion that Bulaj et al. and Keire et al. describe the measurement of reactivity and kinetics of various disulfide bonds but provide no teaching or motivation for a compound for inserting into an organism having a disulfide bond that cleaved more rapidly than oxidized glutathione. Bulaj et al. provides a section headlined: *Possible Applications* (page 8971, second column). The first sentence of this section states, "The results presented here suggest ways in which thiol-disulfide exchange rates might be manipulated advantageously for different purposes." Bulaj et al. go on to suggest ways in which the information they present may be used in protein folding, modeling and synthesis.

Keire et al., in the discussion on page 126 (first column bottom paragraph), state, "The main objective of this research has been to quantitatively characterize the oxidation-reduction chemistry of thiol groups in molecules of biological importance." More specifically, Keire et al. are interested in understanding how the cell maintains "the intracellular distribution of glutathione, coenzyme A, cysteine, and other thiols among their reduced and oxidized forms." They conclude "that the relationships derived in this study can be used to predict redox properties on biological thios" (page 127, final paragraph before *Experimental Section*).

Applicants' believe that while the teachings of Bulaj et al. and Keire et al. would be useful in determining the rate at which a thiol may be cleaved relative to other thiols in a cell, they provide no teaching or motivation to make a compound for inserting into an organism having a disulfide bond that is cleaved more rapidly than oxidized glutathione.

Claims 1, 2, 5, 6 and 13 have been rejected under 35 USC 102(e) as being anticipated by Stein et al. (6,258,774 B1). As the Office Action states, Stein et al. in figure 1, shows a disulfide bond that is cleaved more rapidly that oxidized glutathione. However, this bond is shown as a starting material component and is not present in the compound which is to be delivered to the cell. The disulfide bond present in the compound to be delivered to a cell as taught by Stein et al. is not a labile bond that is cleaved more rapidly than oxidized glutathione as taught by the Applicants. The disulfide bond taught by Stein et al.:
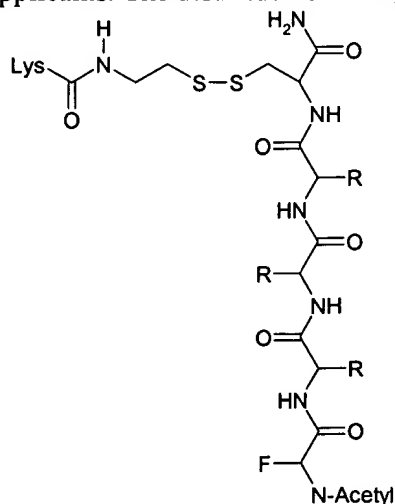
is not a disulfide bond that is cleaved more rapidly than oxidized glutathione. (note: Applicants can not find within the Stein et al. specification identification of "FR$_3$C." A search

5

of the literature revealed a publication by the inventors of 6,258,774, in which the same figure is used (Bioconjugate Chemistry 1998 9(5):612-617). In this publication, FR$_3$C is indicated to be the synthetic peptide N-acetyl-Phe-Arg-Arg-Arg-Cys-NH$_2$.) The Applicants teach, on page 2 lines 16-30 of the specification, that acylating an amine nitrogen two atoms from the sulfur atom increases the pKa of the thiol. The structure shown by Stein et al. shows amide nitrogens (acylated nitrogens) on either side of the disulfide bond. In fact, Stein et al. teach away from using a disulfide bond that is more labile than the bond shown above. Stein et al. teach at column 10 line 28: "Applicants have also discovered that the release rate of a therapeutic agent from a carrier of the present invention can be modulated, depending on the steric hindrance of the thiol compound of the carrier. In particular, Applicants have discovered that the greater the steric hindrance of the thiol compound, the slower the release rate of the therapeutic agent from the carrier" (underline added). Stein et al. then describe attachment of functional groups to sterically hinder to the disulfide bond and reduce its rate of reduction.
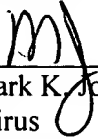
Stein et al. do not teach a labile disulfide bond attached to a transduction signal. Stein et al. teach a TAT peptide but not a transduction signal. The TAT peptide, as taught by Stein et al. consists of a transcription inhibitor, column 2 line 51 to column 3 line 34. More specifically, Stein et al. teach a "Tat inhibitory polypeptide" which interferes with the TAT protein transcription activator.

Stein et al. also teach a "cell uptake promoter." It is the Applicants' opinion that the cell uptake promoter, as taught by Stein et al. is not equivalent to a transduction peptide. Rather, the cell uptake promoter of Stein et al. is equivalent to a targeting group as taught by the Applicants. The only example that Stein et al. provide for a cell uptake promoter is the vitamin biotin (vitamin H). Applicants teach on page 24 lines 8-29 that "folate and other vitamins can also be used for targeting." Holladay et al. 1999 (Biochimica et Biophysica Acta 1426:195-2040) also teach that biotin can be used as a targeting ligand (page 195, abstract and column 2). Targeting groups enhance cell binding and endocytosis (i.e. internalization). This route of cell entry is distinct from that proposed for transduction peptides. Applicants know of no reports in which it is suggested that biotin is able to transport itself and attached molecules directly across membranes.
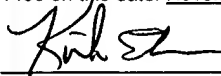
Claims 1, 5, 6, and 13 have been rejected under 35 USC 102(e) as being anticipated by Monahan et al. US Patent 6,429,200B1. The priority date for Monahan et al. is July 17, 1998. The instant application is a continuation-in-part of US Application serial no. 09/312,351 which has a priority date of May 16, 1998, prior to US Patent 6,429,200B1.

The Examiner's objections and rejections are now believed to be overcome by this response to the Office Action. In view of Applicants' amendment and arguments, it is submitted that claims 1-6 and 13 should be allowable.

Respectfully submitted,

Mark K. Johnson   Reg. No. 35,909
Mirus
505 South Rosa Road
Madison, WI 53719
608-238-4400

The design, synthesis, and evaluation of molecules that enable or enhance cellular uptake: Peptoid molecular transporters

Paul A. Wender*†‡, Dennis J. Mitchell§, Kanaka Pattabiraman†, Erin T. Pelkey†, Lawrence Steinman§, and Jonathan B. Rothbard*¶

Departments of †Chemistry and §Neurology, Stanford University, Stanford, CA 94305-5080; and ¶Cellgate Inc., 552 Del Rey Avenue, Sunnyvale, CA 94086

Certain proteins contain subunits that enable their active translocation across the plasma membrane into cells. In the specific case of HIV-1, this subunit is the basic domain Tat_{49-57} (RKKRRQRRR). To establish the optimal structural requirements for this translocation process, and thereby to develop improved molecular transporters that could deliver agents into cells, a series of analogues of Tat_{49-57} were prepared and their cellular uptake into Jurkat cells was determined by flow cytometry. All truncated and alanine-substituted analogues exhibited diminished cellular uptake, suggesting that the cationic residues of Tat_{49-57} play a principal role in its uptake. Charge alone, however, is insufficient for transport as oligomers of several cationic amino acids (histidine, lysine, and ornithine) are less effective than Tat_{49-57} in cellular uptake. In contrast, a 9-mer of L-arginine (R9) was 20-fold more efficient than Tat_{49-57} at cellular uptake as determined by Michaelis–Menton kinetic analysis. The D-arginine oligomer (r9) exhibited an even greater uptake rate enhancement (>100-fold). Collectively, these studies suggest that the guanidinium groups of Tat_{49-57} play a greater role in facilitating cellular uptake than either charge or backbone structure. Based on this analysis, we designed and synthesized a class of polyguanidine peptoid derivatives. Remarkably, the subset of peptoid analogues containing a six-methylene spacer between the guanidine head group and backbone (N-hxg), exhibited significantly enhanced cellular uptake compared to Tat_{49-57} and even to r9. Overall, a transporter has been developed that is superior to Tat_{49-57}, protease resistent, and more readily and economically prepared.

The bioavailability of drugs or molecular probes directed at intracellular receptors depends significantly on their being sufficiently polar for administration and distribution and sufficiently nonpolar for passive diffusion through the relatively nonpolar bilayer of the cell. As a consequence, although covering a broad range of structural diversity, most drugs are limited to a narrow range of physical properties. In addition, many promising drug candidates fail to advance clinically because they fall out of this range, being either too nonpolar for administration and distribution or too polar for passive cellular entry. Exceptions arise mainly through significant changes in formulation [e.g., poorly soluble taxol is formulated in ethanol:Cremophor EL (1)] or extensive tuning of physical properties [e.g., polar oligonucleotides modified with lipid groups (2)]. Several techniques have been developed to enable cellular uptake including drug incorporation into cationic liposomes (3), dendrimers (4), or siderophores (5).

In contrast to most drugs, certain naturally occurring macromolecules enter cells through an active transport mechanism. One important example is the nuclear transcription activator protein (Tat) encoded by HIV type 1 (HIV-1), a 101-aa protein that is required for viral replication (6, 7). Of particular interest for drug delivery is that exogenously added HIV-1 Tat efficiently crosses the plasma membranes of cells in an apparent energy-dependent fashion, localizes to the nucleus, and is functional, stimulating HIV-long terminal repeat-driven RNA synthesis

(6–11). The sequence responsible for the cellular uptake of HIV-1 Tat consists of the highly basic region, amino acid residues 49–57 (RKKRRQRRR) (12–16). The detailed mechanism for the cellular uptake of HIV-1 Tat_{49-57} remains unknown.

HIV-1 Tat has been used to deliver functional biomolecules into cells. Although the entire protein can be used for this purpose, it is more efficient to use the truncated sequence containing only the basic residues required for transport, Tat_{49-57}. Through covalent attachment to $Tat._{49-57}$, several proteins have been delivered into cells, including an inhibitor of human papillomavirus type 16 (HPV-16) (13), ovalbumin into the MHC class I pathway (17), the Cdk inhibitors p27^{Kip1} (18) and p16^{INK4a} (19), and a caspase-3 protein (20). Tat_{49-57} has also been successfully used to deliver β-galactosidase *in vivo* into all tissues of the mouse including the brain (21). In addition to Tat_{49-57}, several other short peptide sequences have been identified with membrane translocation activity, including those derived from Antennapedia (6, 22), fibroblast growth factor (23), Galparan (transportan) (24), and HSV-1 structural protein VP22 (25).

A structural analogy can be drawn between Tat_{49-57} and homopolymers [molecular weight (m.w.) = 4,000–200,000] of the cationic amino acids lysine (26), ornithine (27), and arginine (27) that are also able to enter cells. Polylysine (PL) has been used to efficiently deliver a range of biomolecules into cells including albumin and horseradish peroxidase (PL m.w. = 6700) (28), methotrexate (PL m.w. = 70,000) (29), oligonucleotides (PL m.w. = 14,000) (30), and adenovirus (PL m.w. = 20,500) (31). In addition, polylysine peptoid derivatives (32) have been used for gene delivery. Polyarginine (PA) has also been used to enhance the cellular uptake of tumor antigens (TA). The polyarginine-TA (PA m.w. = 100,000) conjugates are more efficiently translocated into cells than the corresponding polylysine-TA (PL m.w. = 94,000) conjugates by a factor of 10 as determined by fluorescent flow cytometry (33). However, problems related to toxicity, protein precipitation, and cost prevent such large cationic polymers from being broadly useful therapeutically. Because of the potential structural analogy to Tat_{49-57}, we previously compared the cellular uptake of short oligomers of arginine, lysine, ornithine, and histidine. Interestingly, short oligomers of arginine were much more efficient at entering cells than the corresponding short oligomers of histidine, lysine, and ornithine (34).

BIOCHEMISTRY

Prompted by the potential broad value of using molecular transporters to enable or enhance drug delivery, we initiated a program aimed at elucidating the structural features of Tat$_{49-57}$ that are required for its cellular entry. The second and more important goal of this study was to design and synthesize simpler and more effective molecular transporters for use in drug or probe delivery, a goal of broad fundamental and applied consequence.

Materials and Methods

General. Rink amide resin and Boc$_2$O were purchased from NovaBiochem. Diisopropylcarbodiimide, bromoacetic acid, fluorescein isothiocyanate (FITC-NCS), ethylenediamine, 1,3-diaminopropane, 1,4-diaminobutane, 1,6-diaminohexane, 1,8-diaminooctane, *trans*-1,6-diaminocyclohexane, and pyrazole-1-carboxamidine were all purchased from Aldrich. All solvents and other reagents were purchased from commercial sources and used without further purification. The mono-Boc amines were synthesized from the commercially available diamines by using a literature procedure (10 equiv of diamine and 1 equiv of Boc$_2$O in chloroform followed by an aqueous work up to remove unreacted diamine) (35).

N-*tert*-butoxycarbonyl-1,6-*trans*-diaminocyclohexane. Mp 159–161°C; ^{1}H NMR (CDCl$_3$) δ 4.35 (br s, 1H), 3.37 (br s, 1H), 2.61 (br s, 1H), 1.92–2.02 (m, 2H), 1.81–1.89 (m, 2H), 1.43 (s, 9H), 1.07–1.24 (m, 4H) ppm; ^{13}C NMR (D$_6$-DMSO) δ 154.9, 77.3, 49.7, 48.9, 35.1, 31.4, 28.3 ppm; ES-MS (M+1) calcd 215.17, found 215.22.

General Procedure for Peptide Synthesis. Tat$_{49-57}$ (RKKRRQRRR), truncated and alanine-substituted peptides derived from Tat$_{49-57}$, Antennapedia$_{43-58}$ (RQIKIWFQNRRMKWKK), and homopolymers of L-arginine (R5-R9) and D-arginine (r5-r9) were prepared with an automated peptide synthesizer (ABI433) by using standard solid-phase fluorenylmethoxycarbonyl (Fmoc) chemistry (36) with HATU as the peptide coupling reagent. The fluorescein moiety (Fl) was attached via an aminohexanoic acid spacer by treating a resin-bound peptide (1.0 mmol) with FITC (1.0 mmol) and diisopropyl ethyl amine (5 mmol) in dimethylformamide (DMF; 10 ml) for 12 h. Cleavage from the resin was achieved by using 95:5 trifluoroacetic acid (TFA)/triisopropylsilane. Removal of the solvent *in vacuo* gave a crude oil that was triturated with cold ether. The crude mixture thus obtained was centrifuged, the ether was removed by decantation, and the resulting orange solid was purified by RP-HPLC (H$_2$O/CH$_3$CN in 0.1% TFA). The products were isolated by lyophilization and characterized by electrospray mass spectrometry. The purity of the peptides was >95% as determined by analytical RP-HPLC (H$_2$O/CH$_3$CN in 0.1% TFA).

General Procedure for Peptoid Polyamine Synthesis. Peptoids were synthesized manually by using a fritted glass apparatus and positive nitrogen pressure for mixing the resin following the literature procedure developed by Zuckermann (32, 37, 38). Treatment of Fmoc-substituted Rink amide resin (0.2 mmol) with 20% piperidine/DMF (5 ml) for 30 min (2×) gave the free resin-bound amine that was washed with DMF (3 × 5 ml). The resin was treated with a solution of bromoacetic acid (2.0 mmol) and diisopropylcarbodiimide (2.0 mmol) in DMF (5 ml) for 30 min. This procedure was repeated. The resin was then washed (3 × 5 ml DMF) and treated with a solution of mono-Boc diamine (8.0 mmol) in DMF (5 ml) for 12 h. These two steps were repeated until an oligomer of the required length was obtained (Note: the solution of mono-Boc diamine in DMF could be recycled without appreciable loss of yield). The resin was then treated with *N*-Fmoc-aminohexanoic acid (2.0 mmol) and DIC (2.0 mmol) in DMF for 1 h and this was repeated. The Fmoc moiety was then removed by treatment

with 20% piperidine/DMF (5 ml) for 30 min. This step was repeated and the resin was washed with DMF (3 × 5 ml). The resin was then treated with FITC (0.2 mmol) and diisopropyl ethyl amine (2.0 mmol) in DMF (5 ml) for 12 h. The resin was then washed with DMF (3 × 5 ml) and dichloromethane (5 × 5 ml). Cleavage from the resin was achieved by using 95:5 TFA/triisopropylsilane (8 ml). Removal of the solvent *in vacuo* gave a crude oil that was triturated with cold ether (20 ml). The crude mixture thus obtained was centrifuged, the ether was removed by decantation, and the resulting orange solid was purified by RP-HPLC (H$_2$O/CH$_3$CN in 0.1% TFA). The products were isolated by lyophilization and characterized by electrospray mass spectrometry and in selected cases by ^{1}H NMR spectroscopy.

General Procedure for Perguanidinylation of Peptoid Polyamines. A solution of peptoid amine (0.1 mmol) dissolved in deionized water (5 ml) was treated with sodium carbonate (5 equiv per amine residue) and pyrazole-1-carboxamidine (5 equiv per amine residue) and heated at 50°C for 24–48 h. The crude mixture was then acidified with TFA (0.5 ml) and directly purified by RP-HPLC (H$_2$O/CH$_3$CN in 0.1% TFA). The products were characterized by electrospray mass spectrometry and isolated by lyophilization and further purified by RP-HPLC. The yield for the perguanidinylated peptoids was 60–70%, and their purity was >95% as determined by analytical RP-HPLC (H$_2$O/ CH$_3$CN in 0.1% TFA).

Cellular Uptake Assay. The arginine homopolymers and guanidine-substituted peptoids were each dissolved in PBS buffer (pH 7.2), and their concentration was determined by absorption of fluorescein at 490 nm (ε = 67,000). The accuracy of this method for determining transporter concentration was established by weighing selected samples and dissolving them in a known amount of PBS buffer. The concentrations determined by UV spectroscopy correlated with the amounts weighed out manually. Jurkat cells (human T cell line), murine B cells (CH27), or human PBL cells were grown in 10% FCS and DMEM and each of these were used for cellular uptake experiments. Varying amounts of arginine and oligomers of guanidine-substituted peptoids were added to approximately 3 × 10^6 cells in 2% FCS/PBS (combined total of 200 µl) and placed into microtiter plates (96-well) and incubated for varying amounts of time at 23°C or 4°C. The microtiter plates were centrifuged and the cells were isolated, washed with cold PBS (3 × 250 µl), incubated with 0.05% trypsin/0.53 mM EDTA at 37°C for 5 min, washed with cold PBS, and resuspended in PBS containing 0.1% propidium iodide. The cells were analyzed by using fluorescent flow cytometry (FACScan; Becton Dickinson) and cells staining with propidium iodide were excluded from the analysis. The data presented are the mean fluorescent signal for the 5,000 cells collected.

Inhibition of Cellular Uptake with Sodium Azide. The assays were performed as previously described with the exception that the cells used were preincubated for 30 min with 0.5% sodium azide in 2% FCS/PBS buffer before the addition of fluorescent peptides and the cells were washed with 0.5% sodium azide in PBS buffer. All of the cellular uptake assays were run in parallel in the presence and absence of sodium azide.

Cellular Uptake Kinetics Assay. The assays were performed as previously described except the cells were incubated for 0.5, 1, 2, and 4 min at 4°C in triplicate in 2% FCS/PBS (50 µl) in microtiter plates (96-well). The reactions were quenched by diluting the samples into 2% FCS/PBS (5 ml). The assays were then worked up and analyzed by fluorescent flow cytometry as previously described.
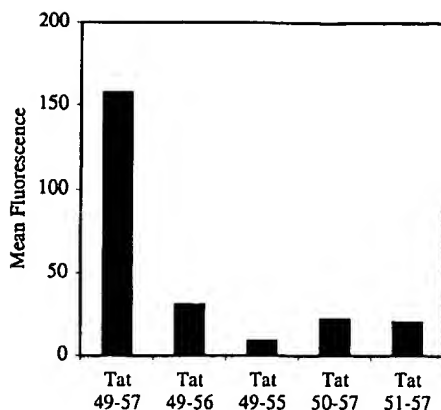
Fig. 1. FACS cellular uptake assay of truncated analogs of Tat_{49-57} (Fl-ahx-RKKRRQRRR): Tat_{49-56} (Fl-ahx-RKKRRQRR), Tat_{49-55} (Fl-ahx-RKKRRQR), Tat_{50-57} (Fl-ahx-KKRRQRRR), and Tat_{51-57} (Fl-ahx-KRRQRRR). Jurkat cells were incubated with varying concentrations (12.5 μM shown) of peptides for 10 min at 23°C.

Results

Structure-Function Relationships of Fluorescently Labeled Peptides Derived from Tat_{49-57}.[||] To determine the structural requirements for the cellular uptake of short arginine-rich peptides, a series of fluorescently labeled truncated analogues of Tat_{49-57} were synthesized by using standard solid-phase chemistry (36). A Fl was attached through an ahx acid spacer on the amino termini. The ability of these fluorescently labeled peptides to enter Jurkat cells was then analyzed by using flow cytometry (Fig. 1). Differentiation between cell surface binding and internalization was accomplished throughout by running a parallel set of assays in the presence and absence of sodium azide. Because sodium azide inhibits energy-dependent cellular uptake (39) but not cell surface binding, the difference in fluorescence between the two assays represents the amount of fluorescence resulting from internalization.

Deletion of one arginine residue from either the amine terminus (Tat_{50-57}) or the carboxyl terminus (Tat_{49-56}) resulted in a significant (80%) loss of intracellular fluorescence relative to the parent sequence (Tat_{49-57}). From the one amino acid truncated analogs, further deletion of R-56 from the carboxyl terminus (Tat_{49-55}) resulted in an additional 60% loss of intracellular fluorescence, whereas deletion of K-50 from the amine terminus (Tat_{51-57}) did not further diminish the amount of internalization. These results indicate that truncated analogs of Tat_{49-57} are significantly less effective at the transcellular delivery of fluorescein into Jurkat cells, and that the arginine residues appear to contribute more to cellular uptake than the lysine residues.

To determine the contribution of individual amino acid residues to cellular uptake, nine fluorescently labeled analogs containing alanine substitutions at each site of Tat_{49-57} were synthesized and assayed by flow cytometry (Fig. 2). Substitution of the noncharged glutamine residue of Tat_{49-57} with alanine (A-54) resulted in a modest decrease in cellular internalization. On the other hand, substitution of each of the cationic residues individually with alanine produced a 70–90% decrease in cellular uptake. In these cases, replacement of lysine (A-50, A-51)
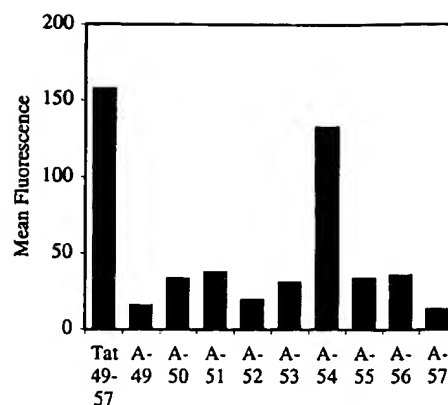

Fig. 2. FACS cellular uptake assay of alanine-substituted analogs of Tat_{49-57}: A-49 (Fl-ahx-AKKRRQRRR), A-50 (Fl-ahx-RAKRRQRRR), A-51 (Fl-ahx-RKAR-RQRRR), A-52 (Fl-ahx-RKKARQRRR), A-53 (Fl-ahx-RKKRAQRRR), A-54 (Fl-ahx-RKKRRARRR), A-55 (Fl-ahx-RKKRRQARR), A-56 (Fl-ahx-RKKRRQRAR), and A-57 (Fl-ahx-RKKRRQRRA). Jurkat cells were incubated with varying concentrations (12.5 μM shown) of peptides for 10 min at 23°C.

or arginine (A-49, A-52, A-55, A-56, A-57) residues with alanine had similar effects in reducing uptake.

To determine whether the chirality of the transporter peptide was important, the corresponding d-isomer (d-Tat_{49-57}) and retro-inverso isomers (l-Tat_{57-49} and d-Tat_{57-49}) were synthesized and assayed by flow cytometry (Fig. 3). Importantly, all three analogs were more effective at entering Jurkat cells than Tat_{49-57}. These results indicated that the chirality of the peptide backbone is not crucial for cellular uptake. Interestingly, the retro-l isomer (Tat_{57-49}), which has three arginine residues located at the amine terminus instead of one arginine and two lysines, found in Tat_{49-57} demonstrated enhanced cellular uptake. Thus, residues at the amine terminus appear to be important and arginines are more effective than lysines for internalization. The improved cellular uptake of the unnatural d-peptides is most likely because of their increased stability to proteolysis in 2% FCS used in the assays. When serum was excluded, the d- and l-peptides were equivalent as expected.

These initial results indicated that arginine content is primarily responsible for the cellular uptake of Tat_{49-57}. Furthermore, these findings are consistent with our previous results showing that short oligomers of arginine are more effective at entering
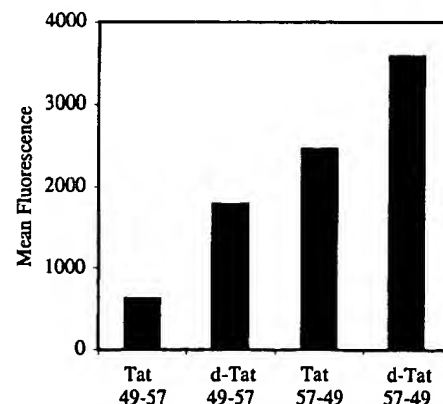

Fig. 3. FACS cellular uptake assay of d- and retro-isomers of Tat_{49-57}: d-Tat_{49-57} (Fl-ahx-rkkrrqrrr), Tat_{57-49} (Fl-ahx-RRRQRRKKR), and d-Tat_{57-49} (Fl-ahx-rrrqrrkkr). Jurkat cells were incubated with varying concentrations (12.5 μM shown) of peptides for 15 min at 23°C.

[||] All synthetic peptides and peptoids contain an aminohexanoic (ahx) acid moiety attached to the N-terminal amino group with a fluorescein moiety (Fl) covalently linked to the amino group of the aminohexanoic acid spacer. The carboxyl terminus of every peptide and peptoid is a carboxamide.
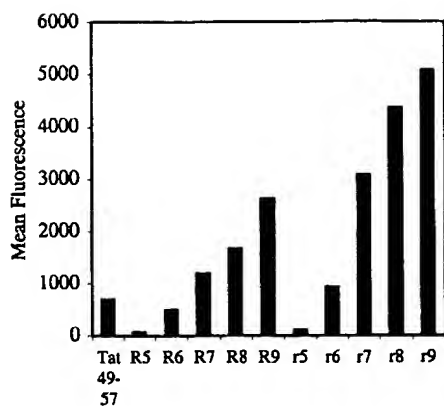
Fig. 4. FACS cellular uptake of a series of arginine oligomers and Tat49-57: R5 (Fl-ahx-RRRRR), R6 (Fl-ahx-RRRRRR), R7 (Fl-ahx-RRRRRRR), R8 (Fl-ahx-RRRRRRRR), R9 (Fl-ahx-RRRRRRRRR), r5 (Fl-ahx-rrrrr), r6 (Fl-ahx-rrrrrr), r7 (Fl-ahx-rrrrrrr), r8 (Fl-ahx-rrrrrrrr), r9 (Fl-ahx-rrrrrrrrr). Jurkat cells were incubated with varying concentrations (12.5 μM shown) of peptides for 15 min at 23°C.

Scheme 1. (a) BrCH$_2$CO$_2$H, DIC, DMF. (b) BocNH-X-NH$_2$, DMF. (c) Fmoc-ahx-CO$_2$H, DIC, DMF. (d) piperidine, DMF. (e) FITC-NCS, DIEA, DMF. (f) 95:5 TFA/TIS. (g) pyrazole-1-carboxamidine, aq. Na$_2$CO$_3$, 50°C. Abbreviations: N-etg, X = (CH$_2$)$_2$; N-arg, X = (CH$_2$)$_3$; N-btg, X = (CH$_2$)$_4$; N-hxg, X = (CH$_2$)$_6$; N-ocg, X = (CH$_2$)$_8$; N-chg, X = trans-1,4-cyclohexyl.
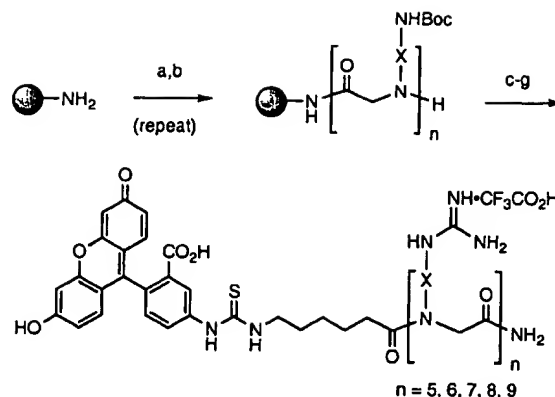
cells than the corresponding short oligomers of lysine, ornithine, and histidine (34). What had not been established was whether arginine homo-oligomers are more effective than Tat49-57. To address this point, Tat49-57 was compared with the L-arginine (R5-R9) and D-arginine (r5-r9) oligomers. Although Tat49-57 contains eight cationic residues, its cellular internalization was between that of R6 and R7 (Fig. 4), indicating that the presence of at least six arginine residues is an important factor for cellular uptake. Significantly, conjugates containing seven to nine arginine residues exhibited better uptake than Tat49-57.

To quantitatively compare the ability of these arginine oligomers and Tat49-57 to enter cells, Michaelis–Menton kinetic analyses were performed. The rates of cellular uptake were determined after incubation (3°C) of the peptides in Jurkat cells for 30, 60, 120, and 240 s (Table 1). The resultant K_m values revealed that R9 entered cells approximately 20-fold faster than Tat47-59. Significantly, the r9 transporter was 100-fold faster than Tat47-59 at entering cells. For comparison, Antennapedia43-58 was also analyzed and was shown to enter cells approximately 2-fold faster than Tat47-59, but significantly slower than r9 or R9.

Design and Synthesis of Peptidomimetic Analogs of Tat49-57. Using the above structure–function relationships obtained with Tat47-59, we designed a series of polyguanidine peptoid derivatives that preserve the 1,4-backbone spacing of side chains of arginine oligomers but have an oligo-glycine backbone devoid of stereogenic centers. These peptoids incorporating arginine-like sides chains on the amide nitrogen were selected because of their expected resistance to proteolysis (40), and potential ease and more significantly lower cost of synthesis (37, 38). Furthermore, racemization, frequently encountered in peptide synthesis, is not a problem in peptoid synthesis and the "submonomer" (38) approach to peptoid synthesis allows for facile modification of side-chain spacers. Although the preparation of an oligourea (41) and peptoid-peptide hybrid (42) derivatives of Tat49-57 have

Table 1. Michaelis–Menton kinetics: Antennapedia43-58 (Fl-ahx-RQIKIWFQNRRMKWKK)

Peptide	K_m, μM	V_{max}
Tat49-57	770	0.38
Antennapedia43-58	427	0.41
R9	44	0.37
r9	7.6	0.38

been previously reported, their cellular uptake was not explicitly studied.

The desired peptoids were prepared by using the "submonomer" (38) approach to peptoids followed by attachment of a Fl through an aminohexanoic acid spacer onto the amine termini.∥ After cleavage from the solid-phase resin, the fluorescently labeled polyamine peptoids thus obtained were converted in good yields (60–70%) into polyguanidine peptoids by treatment with excess pyrazole-1-carboxamidine (43) and sodium carbonate (Scheme 1). Previously reported syntheses of peptoids containing isolated N-Arg units have relied on the synthesis of N-Arg monomers (5–7 steps) before peptoid synthesis and the use of specialized and expensive guanidine protecting groups (Pmc, Pbf) (44, 45). The compounds reported here represent examples of polyguanidinylated peptoids prepared by using a perguanidinylation step. This method provides easy access to polyguanidinylated compounds from the corresponding polyamines and is especially useful for the synthesis of perguanidinylated homooligomers. Furthermore, it eliminates the use of expensive protecting groups (Pbf, Pmc). An additional example of a perguanidinylation of a peptide substrate using a novel triflyl-substituted guanylating agent has recently been reported (46).

The cellular uptake of fluorescently labeled polyguanidine N-arg5,7,9 peptoids was compared with the corresponding D-arginine peptides r5,7,9 (similar proteolytic properties) by using Jurkat cells and flow cytometry. The amount of fluorescence
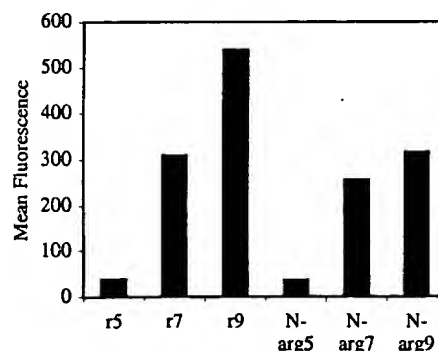
Fig. 5. FACS cellular uptake of polyguanidine peptoids and D-arginine oligomers. Jurkat cells were incubated with varying concentrations (12.5 μM shown) of peptoids and peptides for 4 min at 23°C.
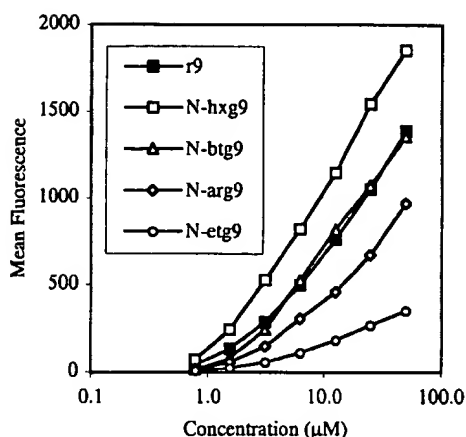
Fig. 6. FACS cellular uptake of D-arginine oligomers and polyguanidine peptoids. Jurkat cells were incubated with varying concentrations (12.5 μM shown) of fluorescently labeled peptoids and peptides for 4 min at 23°C.

measured inside the cells with N-arg5,7,9 was found to be proportional to the number of guanidine residues: N-arg9 > N-arg7 > N-arg5 (Fig. 5), analogous to that found for r5,7,9. Importantly, the N-arg5,7,9 peptoids showed only a slightly lower amount of cellular entry compared with the corresponding peptides, r5,7,9. Hence, it is clear from these results that the hydrogen bonding along the peptide backbone of Tat47–59 or arginine oligomers is not a required structural element for cellular uptake and oligomeric guanidine-substituted peptoids can be used in place of arginine-rich peptides as molecular transporters. The addition of sodium azide inhibited internalization demonstrating that the cellular uptake of peptoids was also energy-dependent.

After establishing that the N-arg peptoids efficiently crossed cellular membranes, the effect of side chain length (number of methylenes) on cellular uptake was investigated. Significantly, for a given number of guanidine residues (5, 7, or 9), cellular uptake was proportional to side-chain length. Peptoids with longer side chains exhibited more efficient cellular uptake with N-hxg9 > N-btg9 > r9 > N-arg9 > N-etg9 (Fig. 6). Of special importance, the N-hxg peptoids showed remarkably high cellular uptake, even greater than the corresponding D-arginine oligomers. The cellular uptake of the corresponding heptamers and pentamers also showed the same relative trend. The longer side chains embodied in the N-hxg peptoids improved the cellular uptake to such an extent that the amount of internalization was comparable to the corresponding D-arginine oligomer containing one more guanidine residue (Fig. 7). For example, the N-hxg7 peptoid showed comparable cellular uptake to r8.

To address whether the increase in cellular uptake was because of the hydrophobic nature or the flexibility of the side chains, a set of peptoids was synthesized containing cyclohexyl side chains, N-chg5,7,9 peptoids. These contain the same number of side-chain carbons as the N-hxg peptoids but possess different degrees of freedom. Interestingly, the N-chg peptoid showed much lower cellular uptake activity than all of the previously assayed peptoids, including the N-etg peptoids (Fig. 8). Therefore, the conformational flexibility and sterically unencumbered nature of the straight chain alkyl spacing groups is important for efficient cellular uptake.

Discussion

The nona-peptide, Tat49–57, has been shown to translocate efficiently across plasma membranes (14). The goal of this research was to determine the structural basis for this activity and to use this information to develop simpler and more effective
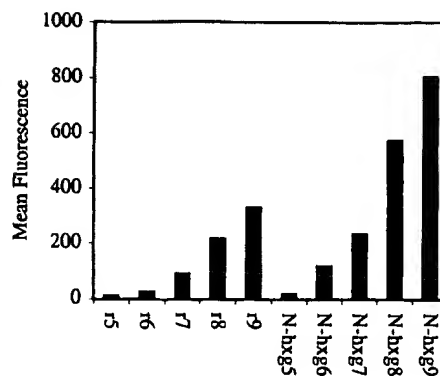

Fig. 7. FACS cellular uptake of D-arginine oligomers and N-hxg peptoids. Jurkat cells were incubated with varying concentrations (6.3 μM shown) of fluorescently labeled peptoids and peptides for 4 min at 23°C.

molecular transporters. Toward this end, truncated and alanine substituted derivatives of Tat49–57 conjugated to a fluorescein label were prepared. These derivatives exhibited greatly diminished cellular uptake compared with Tat49–57, indicating that all of the cationic residues of Tat49–57 are required for efficient cellular uptake. When compared with our previous studies on short oligomers of cationic peptides (34), these findings suggested that an oligomer of arginine might be superior to Tat49–57 and certainly more easily and cost-effectively prepared. Comparison of short arginine oligomers with Tat49–57 showed that members of the former were indeed more efficiently taken up into cells. This was quantified further by Michaelis–Menton kinetics analysis that showed that the R9 and r9 oligomers had K_m values 20-fold and 100-fold greater than that found for Tat49–57.

Given the importance of the guanidino head group and the apparent insensitivity of the oligomer chirality revealed in our peptide studies, we designed and synthesized a series of polyguanidine peptoids. The peptoids N-arg5,7,9, incorporating the arginine side chain, exhibited comparable cellular uptake to the corresponding d-arginine peptides r5,7,9, indicating that the hydrogen bonding along the peptide backbone and backbone chirality are not essential for cellular uptake. This observation is consistent with molecular models of these peptoids, arginine oligomers, and Tat49–57, all of which have a deeply embedded backbone and a guanidinium dominated surface. Molecular models further reveal that these structural characteristics are retained in varying degree in oligomers with different alkyl spacers between the peptoid backbone and guanidino head
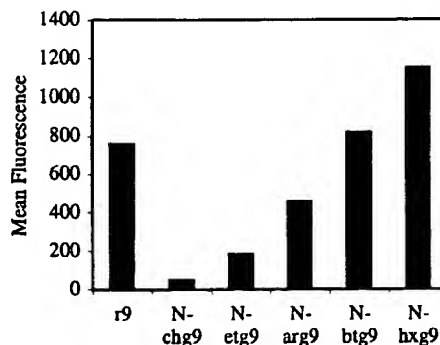

Fig. 8. FACS cellular uptake of D-arginine oligomers and N-chg peptoids. Jurkat cells were incubated with varying concentrations (12.5 μM shown) of fluorescently labeled peptoids and peptides for 4 min at 23°C.

groups. Accordingly, a series of peptoids incorporating 2- (N-etg), 4- (N-btg), and 6-atom (N-hxg) spacers between the backbone and side chain were prepared and compared for cellular uptake with the N-arg peptoids (3-atom spacers) and D-arginine oligomers. The length of the side chains had a dramatic effect on cellular entry. The amount of cellular uptake was proportional to the length of the side chain with N-hxg > N-btg > N-arg > N-etg. Cellular uptake was improved when the number of alkyl spacer units between the guanidine head group and the backbone was increased. Significantly, N-hxg9 was superior to r9, the latter being 100-fold better that Tat$_{49-57}$. This result led us to prepare peptoid derivatives containing longer octyl spacers (N-ocg) between the guanidino groups and the backbone. Issues related to solubility prevented us from testing these compounds.

Because both perguanidinylated peptides and perguanidinylated peptoids efficiently enter cells, the guanidine head group (independent of backbone) is apparently a critical structural determinant of cellular uptake. However, the presence of several (over six) guanidine moieties on a molecular scaffold is not sufficient for active transport into cells as the N-chg peptoids did not efficiently translocate into cells. Thus, in addition to the guanidine head group, the conformational mobility of designed transporters also plays a role in cellular uptake.

In summary, this investigation identified a series of structural characteristics including sequence length, amino acid composition, and chirality that influence the ability of Tat$_{49-57}$ to enter cells. These characteristics provided the blueprint for the design of a series of peptoids, of which 17 members were synthesized and assayed for cellular uptake. Significantly, the N-hxg9 transporter was found to be superior in cellular uptake to r9 which in turn was comparable to N-btg9. Hence, these peptoid transporters proved to be substantially better then Tat$_{49-57}$. This research established that the peptide backbone and hydrogen bonding along that backbone are not required for cellular uptake, that the guanidino head group is superior to other cationic subunits, and most significantly, that an extension of the alkyl chain between the backbone and the head group provides superior transporters. In addition to better uptake performance, these peptoids offer several advantages over Tat$_{49-57}$ including cost-effectiveness, ease of synthesis of analogs, and protease stability. These features along with their significant water solubility (>100 mg/ml) indicate that these peptoids could serve as effective transporters for the molecular delivery of drugs, drug candidates, and other agents into cells.

1. Terwogt, J. M. M., Nuijen, B., Huinink, W. W. T. B. & Beignen, J. H. (1997) *Cancer Treat. Rev.* **23**, 87–95.
2. Rait, A., Pirollo, K., Will, D. W., Peyman, A., Rait, V., Uhlmann, E. & Chang, E. H. (2000) *Bioconjugate Chem.* **11**, 153–160.
3. Rui, Y. J., Wang, S., Low, P. S. & Thompson, D. H. (1998) *J. Am. Chem. Soc.* **120**, 11213–11218.
4. Kono, K., Liu, M. & Fréchet, J. M. J. (1999) *Bioconjugate Chem.* **10**, 1115–1121.
5. Ghosh, A., Ghosh, M., Niu, C., Malouin, F., Moellmann, U. & Miller, M. J. (1996) *Chem. Biol.* **3**, 1011–1019.
6. Lindgren, M., Hällbrink, M., Prochiantz, A. & Langel, Ü. (2000) *Trends Pharmacol. Sci.* **21**, 99–103.
7. Jeang, K.-T., Xiao, H. & Rich, E. A. (1999) *J. Biol. Chem.* **274**, 28837–28840.
8. Green, M. & Loewenstein, P. M. (1988) *Cell* **55**, 1179–1188.
9. Frankel, A. D. & Pabo, C. O. (1988) *Cell* **55**, 1189–1193.
10. Mann, D. A. & Frankel, A. D. (1991) *EMBO J.* **10**, 1733–1739.
11. Vivés, E., Charneau, P., Van Rietschoten, J., Rochat, H. & Bahraoui, E. (1994) *J. Virol.* **68**, 3343–3353.
12. Vivés, E., Granier, C., Prevot, P. & Leblue, B. (1997) *Lett. Pept. Sci.* **4**, 429–436.
13. Pepinsky, R. B., Androphy, E. J., Corina, K., Brown, R. & Barsoum, J. (1994) *DNA Cell Biol.* **13**, 1011–1019.
14. Vivés, E., Brodin, P. & Lebleu, B. (1997) *J. Biol. Chem.* **272**, 16010–16017.
15. Fawell, S., Seery, J., Daikh, T., Moore, C., Chen, L. L., Pepinsky, B. & Barsoum, J. (1994) *Proc. Natl. Acad. Sci. USA* **91**, 664–668.
16. Anderson, D. C., Nichols, E., Manger, R., Woodle, D., Barry, M. & Fritzberg, A. R. (1993) *Biochem. Biophys. Res. Commun.* **194**, 876–884.
17. Kim, D. T., Mitchell, D. J., Brockstedt, D. G., Fong, L., Nolan, G. P., Fathman, C. G., Engelman, E. G. & Rothbard, J. B. (1997) *J. Immunol.* **159**, 1666–1668.
18. Nagahara, H., Vocero-Akbani, A. M., Snyder, E. L., Ho, A., Latham, D. G., Lissy, N. A., Becker-Hapak, M., Ezhevsky, S. A. & Dowdy, S. F. (1998) *Nat. Med.* **4**, 1449–1452.
19. Gius, D. R., Ezhevsky, S. A., Becker-Hapak, M., Nagahara, N., Wei, M. C. & Dowdy, S. F. (1999) *Cancer Res.* **59**, 2577–2580.
20. Vocero-Akbani, A. M., Vander-Heyden, N., Lissy, N. A., Ratner, L. & Dowdy, S. F. (1999) *Nat. Med.* **5**, 29–33.
21. Schwarze, S. R., Ho, A., Vocero-Akbani, A. & Dowdy, S. F. (1999) *Science* **285**, 1569–1572.
22. Derossi, D., Chassaing, G. & Prochiantz, A. (1998) *Trends Cell Biol.* **8**, 84–87.
23. Lin, Y.-Z., Yao, S., Veach, R. A., Torgerson, T. R. & Hawiger, J. (1995) *J. Biol. Chem.* **270**, 14255–14258.
24. Pooga, M., Hällbrink, M., Zorko, M. & Langel, U. (1998) *FASEB J.* **12**, 67–77.
25. Elliott, G. & O'Hare, P. (1997) *Cell* **88**, 223–233.
26. Ryser, H. J.-P. (1967) *Nature (London)* **215**, 934–936.
27. Emi, N., Kidoaki, S., Yoshikawa, K. & Saito, H. (1997) *Biochem. Biophys. Res. Commun.* **231**, 421–424.
28. Shen, W.-C. & Ryser, H. J.-P. (1978) *Proc. Natl. Acad. Sci. USA* **75**, 1872–1876.
29. Ryser, H. J.-P. & Shen, W.-C. (1978) *Proc. Natl. Acad. Sci. USA* **75**, 3867–3870.
30. Leonetti, J.-P., Degols, G. & Lebleu, B. (1990) *Bioconjugate Chem.* **1**, 149–153.
31. Mulders, P., Pang, S., Dannull, J., Kaboo, R., Hinkel, A., Michel, A., Tso, C.-L., Roth, M. & Belldegrun, A. (1998) *Cancer Res.* **58**, 956–961.
32. Murphy, J. E., Uno, T., Hamer, J. D., Dwarki, V. & Zuckermann, R. N. (1998) *Proc. Natl. Acad. Sci. USA* **95**, 1517–1522.
33. Buschle, M., Schmidt, W., Zauner, W., Mechtler, K., Trska, B., Kirlappos, H. & Birnstiel, M. L. (1997) *Proc. Natl. Acad. Sci. USA* **94**, 3256–3261.
34. Mitchell, D. J., Kim, D. T., Steinman, L. C., Fathman, C. G. & Rothbard, J. B. (2000) *J. Peptide Res.* **55**, in press.
35. Pons, J.-F., Fauchere, J.-L., Lamaty, F., Molla, A. & Lazaro, R. (1998) *Eur. J. Org. Chem.* 853–859.
36. Atherton, E. & Sheppard, R. C. (1989) *Solid-Phase Peptide Synthesis* (IRL, Oxford).
37. Simon, R. J., Kania, R. S., Zuckermann, R. N., Huebner, V. D., Jewell, D. A., Banville, S., Ng, S., Wang, L., Rosenberg, S., Marlowe, C. K., *et al.* (1992) *Proc. Natl. Acad. Sci. USA* **89**, 9367–9371.
38. Zuckermann, R. N., Kerr, J. M., Kent, S. B. H. & Moos, W. H. (1992) *J. Am. Chem. Soc.* **114**, 10646–10647.
39. Sandvig, K. & Olsnes, S. (1982) *J. Biol. Chem.* **257**, 7504–7513.
40. Miller, S. M., Simon, R. J., Ng, S., Zuckermann, R. N., Kerr, J. M. & Moos, W. H. (1994) *Bioorg. Med. Chem. Lett.* **4**, 2657–2662.
41. Tamilarasu, N., Huq, I. & Rana, T. M. (1999) *J. Am. Chem. Soc.* **121**, 1597–1598.
42. Hamy, F., Felder, E. R., Heizmann, G., Lazdins, J., Aboul-Ela, F., Varani, G., Karn, J. & Klimkait, T. (1997) *Proc. Natl. Acad. Sci. USA* **94**, 3548–3553.
43. Bernatowicz, M. S., Wu, Y. L. & Matsueda, G. R. (1992) *J. Org. Chem.* **57**, 2497–2502.
44. Kruijtzer, J. A. W., Hofmeyer, L. J. F., Heerma, W., Versluis, C. & Liskamp, R. M. J. (1998) *Chem. Eur. J.* **4**, 1570–1580.
45. Heizmann, G. & Felder, E. R. (1994) *Peptide Res.* **7**, 328–332.
46. Feichtinger, K., Sings, H. L., Baker, T. J., Matthews, K. & Goodman, M. (1998) *J. Org. Chem.* **63**, 8432–8439.

A Polyethylene Glycol Copolymer for Carrying and Releasing Multiple Copies of Cysteine-Containing Peptides

Shaei-Yun Huang,[†,‡] Shahriar Pooyan,[†,§] Jihong Wang,[†,‡] Indrani Choudhury,[§]
Michael J. Leibowitz,[§,‖] and Stanley Stein*[,†,‡,§]

Center for Advanced Biotechnology and Medicine and Chemistry Department, Rutgers University,
New Brunswick, New Jersey 08903-2101, Department of Molecular Genetics and Microbiology,
Robert Wood Johnson Medical School-UMDNJ, Piscataway, New Jersey 08854, and
Cancer Institute of New Jersey, New Brunswick, New Jersey 08903 . Received April 6, 1998;
Revised Manuscript Received July 6, 1998

Two different methods were developed to prepare an adduct of a poly(ethylene glycol)-lysine copolymer with either cysteamine or 1-amino-2-methyl-2-propanethiol. Cysteine-containing peptides could then be disulfide-linked to the thiol groups on the polymer in a facile manner. In the described procedures, a coupling ratio of about 8 peptides/molecule of poly(ethylene glycol)-lysine copolymer ($M_w = 27\,000$) was typically attained. The products were stable at neutral pH, but the peptides could be released from the polymer in a physiologically relevant reducing environment. The release rate was highly dependent on the linker used for forming the disulfide bond. To illustrate the potential biomedical usefulness of this polymer carrier, a Tat peptide–PEG conjugate was shown to inhibit expression of a reporter gene fused to the TAR element of human immunodeficiency virus in a model cell assay.

INTRODUCTION

Covalent attachment of water-soluble polymers can be used to manipulate the pharmacologic properties of a drug (*1*). Poly(ethylene glycol) (PEG)[1] can be derivatized with various functional groups for appending drug molecules (*2*). For example, appending PEG chains to a protein can increase its circulating half-life and minimize its immunogenic properties (*3*). With regard to low-molecular-weight drugs, Kohn and colleagues have designed a PEG-lysine copolymer having multiple attachment sites (*4*). They then prepared conjugates through either biostable or biodegradable linkages (*4*), but they did not investigate the biodegradable disulfide linkage. The disulfide linkage might be especially useful for drug delivery into cells, due to the stronger reducing environment within cells than in extracellular fluids. Stein and colleagues prepared a PEG derivative having a terminal thiol protected by disulfide linkage with 2-thiopyridine (*5*). They showed its usefulness by making a conjugate with papain, which was linked to PEG through its active-site cysteine residue, thereby keeping this enzyme in an inactive state until release from the polymer by a reducing agent. We now report the preparation and release

properties of a PEG-lysine copolymer having multiple 2-thiopyridine-protected attachment sites for cysteine-containing peptides, including those having appended biotin moieties as cellular uptake enhancers.

MATERIALS AND METHODS

Materials. Cysteamine hydrogen chloride, Ellman's reagent [5,5′-dithiobis(2-nitrobenzoic acid)], and glutathione (reduced form) were obtained from Sigma Chemicals (St. Louis, MO). Dithiothreitol (DTT) was obtained from Pierce (Rockford, IL). 2,2′-Dipyridyl disulfide, 1-amino-2-methyl-2-propanethiol, diisopropylethylamine (DIEA), and silica gel, 70–230 mesh, 60A were obtained from Aldrich Chemical (Milwaukee, WI). Hydroxybenzotriazole (HOBt), benzotriazol-1-yloxytris(dimethylamino)phosphonium hexafluorophosphate (BOP), and dimethylformamide (DMF) were obtained from PerSeptive Biosystems (Boston, MA). Dichloromethane (DCM) and methanol (MeOH) were HPLC grade and obtained from Fisher Scientific (Pittsburgh, PA). Sephadex was obtained from Pharmacia LKB Biotechnology (Piscataway, NJ). Poly(ethylene glycol)-lysine copolymer ($M_w = 2.69 \times 10^4$, 2198/repeating unit), which was synthesized according to a published procedure (*4*), was kindly supplied by John Kemnitzer and Joachim Kohn.

Peptide Synthesis. The peptide *N*-acetyl-Phe-Arg-Arg-Arg-Cys-NH₂ (abbreviated as FR₃C) was synthesized at the Louisiana State University (LSU) core facility using Fmoc chemistry, purified by reversed-phase HPLC, and confirmed for structure by mass spectral analysis. The peptides *N*-acetyl-Arg-Lys-Lys-Arg-Arg-Gln-Arg-Arg-Arg-Cys-NH₂ (Tat9-Cys) and *N*-acetyl-Arg-Lys-Lys-Arg-Arg-Gln-Arg-Arg-Arg-Lys(ε-biotin)-Cys-NH₂ [Tat9K(bio)-Cys] were manually synthesized using Fmoc chemistry. For radiolabeling, the assembled peptide on the solid support was allowed to react with tritiated acetic anhydride in the presence of the coupling activation reagents BOP, HOBt, and DIEA. Acetylation of the peptide was com-

* Corresponding author. E-mail: stein@mbcl.rutgers.edu.
Phone: 732-235-5319. Fax: 732-235-4850.
 † Center for Advanced Biotechnology and Medicine.
  ‡ Chemistry Department.
 § Department of Molecular Genetics and Microbiology.
  ‖ Cancer Institute of New Jersey.
  [1] Abbreviations: BOP, benzotriazol-1-yloxytris(dimethylamino)phosphonium hexafluorophosphate; CAT, chloramphenicol acetyltransferase; DIEA, diisopropylethylamine; DTT, dithiothreitol; FR₃C, *N*-acetyl-Phe-Arg-Arg-Arg-Cys-NH₂; HOBt, hydroxybenzotriazole; LTR, long terminal repeat; PBS, phosphate-buffered saline; PEG, poly(ethylene glycol); Tat9-Cys, *N*-acetyl-Arg-Lys-Lys-Arg-Arg-Gln-Arg-Arg-Arg-Cys-NH₂; Tat9K(bio)Cys, *N*-acetyl-Arg-Lys-Lys-Arg-Arg-Gln-Arg-Arg-Arg-Lys(ε-biotin)-Cys-NH₂.

Scheme 1
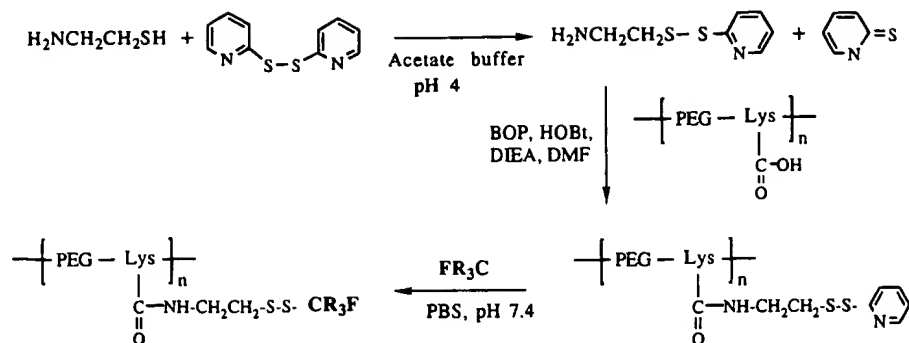
Scheme 2
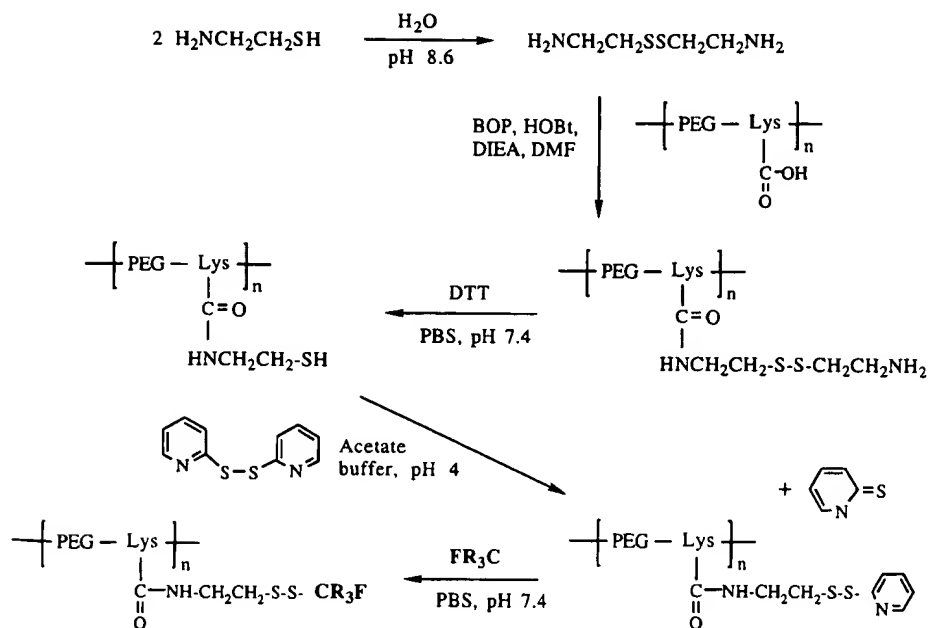
pleted by chasing with an excess of nonradioactive acetic anhydride. After cleavage from the solid support and ether precipitation, the radiolabeled peptide was purified by chromatography on Sephadex G-10 using PBS (0.15 M NaCl, 20 mM potassium phosphate buffer, pH 7.4) for elution.

Preparation of PEG-Cysteamine-TP by Scheme 1. To a solution of cysteamine hydrogen chloride (0.50 g, 4.4 mmol) dissolved in 15 mL of degassed buffer (0.1 N sodium acetate adjusted to pH 4.0 with acetic acid, 0.3 M sodium chloride, and 1 mM EDTA) was added 2,2'-dithiodipyridine (3.5 g, 15 mmol) dissolved in 18 mL of MeOH. The mixture was stirred at room temperature under N_2. The reaction, which was monitored with thin-layer chromatography (ammonium hydroxide/MeOH/DCM, 2/10/90), was complete after 4 h. The MeOH was removed in vacuo and the residue was made basic by saturating with sodium carbonate. The residue was extracted into DCM (3 × 50 mL) and the combined DCM was washed with water (2 × 40 mL) and brine (40 mL) and then dried over magnesium sulfate. The magnesium sulfate was filtered and the filtrate was concentrated in vacuo to an oily residue. The product, cysteamine-TP, was purified by flash chromatography on a silica gel column (ammonium hydroxide/MeOH/DCM, 2/10/90). Yield: 0.30 g (yellow oil) (36%). ^{1}H NMR (CDCl$_3$): δ 8.4–8.5 ppm (m, 1H), 7.7–7.6 ppm (m, 2H), 7.15–7.0 ppm (m, 1H), 3.0–2.7 ppm (m, 4H), 0.9 ppm (b, 2H).

PEG-lysine copolymer (0.20 g, 91 μmol of lysine) was dissolved in 2.5 mL of degassed DMF. Cysteamine-TP (0.5 mmol), BOP (0.5 mmol), HOBt (0.5 mmol), and DIEA (25 μL) were added to the PEG coployr̀ner solution and stirred under N_2 overnight. The product was precipitated with cold ether, washed with cold ether, and then dried by Speedvac (Savant Instrument Co., Farmingdale, NY) to a gellike residue. The product was dissolved and purified on a Sephadex G-75 column (48 mL bed volume) using 0.1 N acetic acid. Appropriate fractions were combined and lyophilized. Yield: 0.11 g (colorless solid).

Preparation of PEG-Cysteamine-TP by Scheme 2. Cysteamine hydrogen chloride was first converted to the disulfide-linked dimer by overnight stirring of an aqueous solution (0.3 g in 15 mL) adjusted to pH 8.6 with triethylamine. Ellman's assay indicated less than 1% remaining free thiol. To the mixture was added a saturated solution of sodium carbonate to pH 10, followed by extracting into DCM (5 × 20 mL), drying over magnesium sulfate, filtering, and concentrating on a rotary evaporator. PEG-lysine copolymer (0.20 g, 91 μmol of lysine) was dissolved in 2.5 mL of degassed DMF. Cysteamine dimer (650 μmol), BOP (650 μmol), HOBt (650 μmol), and DIEA (25 μL) were added to the PEG coploymer solution and stirred under N_2 overnight. The product was precipitated with cold ether, washed with cold ether, and then dried by Speedvac to a gellike residue. The product was purified on a Sephadex G-75

gel filtration column, as above. Appropriate fractions were combined and lyophilized to yield 70 mg of colorless solid, which was dissolved in degassed PBS (pH 7.4). DTT (10 molar equivalents based on lysine) was then added and the reduction reaction proceeded under N_2 overnight. The product was purified on a G-75 column (48 mL bed volume) using 0.1 N acetic acid containing 1 mM EDTA for elution. Appropriate fractions were combined and lyophilized to yield 60 mg of colorless solid, which was dissolved in 4 mL of degassed buffer (0.1 N sodium acetate adjusted to pH 4 with acetic acid, 0.3 M sodium chloride, 1 mM EDTA). 2,2'-Dithiodipyridine (270 μmol) dissolved in 3 mL of degassed MeOH was added, and the reaction mixture was stirred under N_2 for 2 h. The MeOH was removed on a rotary evaporator, and the product was purified on a Sephadex G-75 column (bed volume 48 mL) using 0.1 N acetic acid for elution. Appropriate fractions were combined and lyophilized to yield 30 mg of colorless solid. A similar procedure was used to prepare the PEG derivative of the sterically hindered cysteamine analogue 1-amino-2-methyl-2-propanethiol.

Determination of the 2-Thiopyridine Content in PEG-Cysteamine-TP. The concentration of a PEG-cysteamine-TP solution was determined by acid hydrolysis and measurement of the released lysine using an Applied Biosystems amino acid analyzer (LSU core facility). Varying amounts of PEG-cysteamine-TP (100, 200, and 400 μL) of a 4 mg/mL (ca. 2 μmol/mL of lysine) solution in water were reacted separately with an excess of DTT (200 μL of 26 μmol/mL in water) and diluted to a final volume of 1.0 mL with PBS. The amount of 2-thiopyridone liberated was quantitated using a molar extinction coefficient of 7.06 × 10^3 at 343 nm (*6*).

Preparation of PEG-cysteamine-Peptide. PEG-cysteamine-TP, dissolved in water (8 μmol/mL of lysine), was mixed with an equal volume of PBS containing 1 mM EDTA. To 3 mL of this solution was added 1 equiv [as determined by Ellman's assay for thiols (*7*)] of the peptide FR$_3$C. The reaction, which was monitored by absorbance at 343 nm on aliquots of the mixture, was complete after 15 min of stirring under N_2. The product was purified on a Sephadex G-75 column, using PBS as eluent. Appropriate fractions were pooled. The extent of peptide derivatization of the copolymer was determined by amino acid analysis (LSU core facility). Other combinations of a PEG carrier and a peptide, including radiolabeled peptides, were prepared similarly.

Release of Peptides from PEG—S-S-Peptide Conjugates. The disulfide-linked conjugate PEG-(cysteamine-FR$_3$C)$_n$ was added to a solution of reduced glutathione (3 mM in PBS) to a final peptide concentration of 0.3 mM and then incubated under N_2 at room temperature. A sample was taken at each time point, acidified by adding an aliquot of 5% TFA, and applied to a G-75 column in 0.1% TFA (7 mL bed volume) to separate PEG-conjugated peptide from free peptide. Appropriate fractions in the high-molecular-weight region were pooled, and the extent of peptide derivatization at each time point was determined by amino acid analysis. For measuring the release of radiolabeled peptide, each time point aliquot was acidified to pH 3.5 with sulfuric acid. The PEG-conjugated peptide and the free peptide were then separated using ultrafiltration on Centricon-10 (Amicon/Millipore, Bedford, MA). To ensure complete separation, the retentate was diluted and ultrafiltered two more times. Radioactivity in the retentate and combined filtrate was quantitated by scintillation counting.

Inhibition of Protein Expression from a TAR-CAT Plasmid. Details of this assay have been published (*8*). Briefly, Jurkat cells were stably transfected with a recombinant plasmid comprising the HIV-1 long terminal repeat (LTR), which contains the TAR (transactivator response element) domain, linked to the chloramphenicol acetyltransferase (CAT) gene on the pRep10 episomal vector (Invitrogen, Carlsbad, CA) (S. Stein, B. Beiss, and A. B. Rabson, unpublished results). For expression of Tat protein, which transactivates transcription after binding to the TAR RNA domain of nascent transcripts, cells were transfected with pAR(Tat), which comprises the HIV-1 LTR and viral sequences encoding the 72 amino acid form of Tat. CAT protein in harvested cells was measured using an immunoassay kit from Boehringer-Mannheim (Indianapolis, IN). In this assay, cells were transfected with pAR(Tat) at $t = 0$, and the cells were incubated in 10% fetal calf serum under 95% air/5% carbon dioxide. The Tat-peptide inhibitor, either free or appended to the PEG carrier, was added at various concentrations at $t = 18$ h, and the cells were harvested for CAT immunoassay at $t = 42$ h.
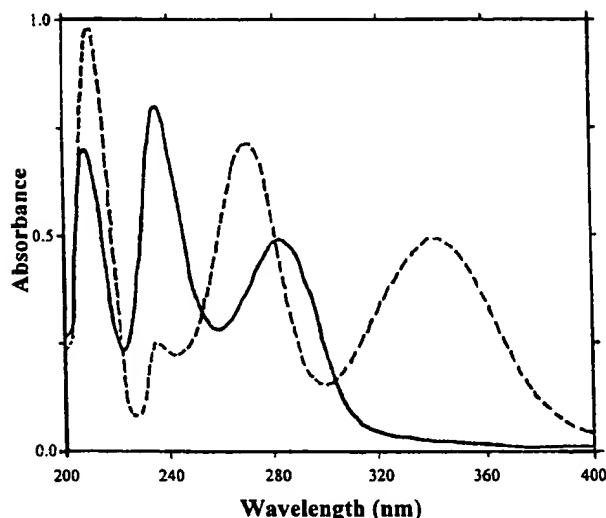
RESULTS

Preparation of PEG—S-S-Peptides. The synthetic routes are given in Schemes 1 and 2. In Scheme 1, cysteamine was first converted into the mixed disulfide with 2-thiopyridine. The cysteamine-TP reagent was purified by silica gel chromatography, and its structure was confirmed by ^{1}H NMR. It was necessary to use this reagent immediately for coupling to the PEG-lysine copolymer, since the 2-thiopyridine group would react back to 2,2'-dipyridyl disulfide, as evaluated by NMR, at a rate of about 15%/day. Amide bond formation between the carboxylate groups on the PEG-lysine copolymer and the amino group on cysteamine was accomplished using reagents typically used for coupling in peptide synthesis (Scheme 1). In Scheme 2, cysteamine was first converted to the symmetric disulfide, then appended to the PEG-lysine copolymer, and finally converted to the 2-thiopyridine derivative. Preparation of the PEG-1-amino-2-methyl-2-propanethiol-TP derivative by Scheme 2 was as facile as that of the cysteamine version.

The disulfide bond between 2-thiopyridine and cysteamine appended to PEG was stable to cleavage in PBS (pH 7.4), as determined by absence of absorbance at 343 nm after 24 h at room temperature. However, upon addition of a cysteinyl-peptide, FR$_3$C, reaction was complete within several minutes, as determined by the released 2-thiopyridone measured at 343 nm (Figure 1). This coupling reaction was about 100 times slower for the polymer in which 1-amino-2-methyl-2-propanethiol was substituted for cysteamine.

To determine the stoichiometry, the amount of 2-thiopyridone released from a given amount of PEG-cysteamine-TP solution by an excess of reducing agent (DTT) in PBS was measured. Then, 1 equiv (as defined by thiol groups measured by Ellman's assay) of the peptide, FR$_3$C, was added to an aliquot of PEG-cysteamine-TP solution, and essentially complete release of 2-thiopyridone was observed. Purification of the product, PEG—S-S-peptide, by gel filtration chromatography gave complete separation from released 2-thiopyridone and, presumably, from any residual unreacted peptide (Figure 2).

Acid hydrolysis, followed by amino acid analysis, was used to determine the concentration of the PEG-lysine

Figure 1. Spectroscopic analysis of the reaction of PEG-cysteamine-TP with the peptide FR₃C. The UV spectrum of a solution of PEG-cysteamine-TP is shown (solid line). Addition of the peptide results in release of 2-thiopyridone, which is observed as a peak with a maximum at 343 nm (dashed line).

copolymer, and treatment with an excess of DTT was used to determine the amount of coupled cysteamine-TP on that same sample. By this procedure, it was determined that 66 ± 8% of the lysine carboxylate groups had been derivatized with cysteamine-TP on a sample of PEG-cysteamine-TP prepared by Scheme 1. Acid hydrolysis, followed by amino acid analysis was also used to determine the extent of derivatization by the peptide, FR₃C. Duplicate analyses gave a ratio of Phe:Lys of 0.64 and 0.55 and a ratio of Arg:Lys of 2.0 and 1.8. Therefore, the extent of peptide derivatization, based on lysine groups in the copolymer backbone, was 62 ± 4%. In another sample prepared by Scheme 1, the peptide coupling ratio was found to be 66 ± 5%. In a sample prepared by Scheme 2, the peptide coupling ratio was found to be 78 ± 9%.
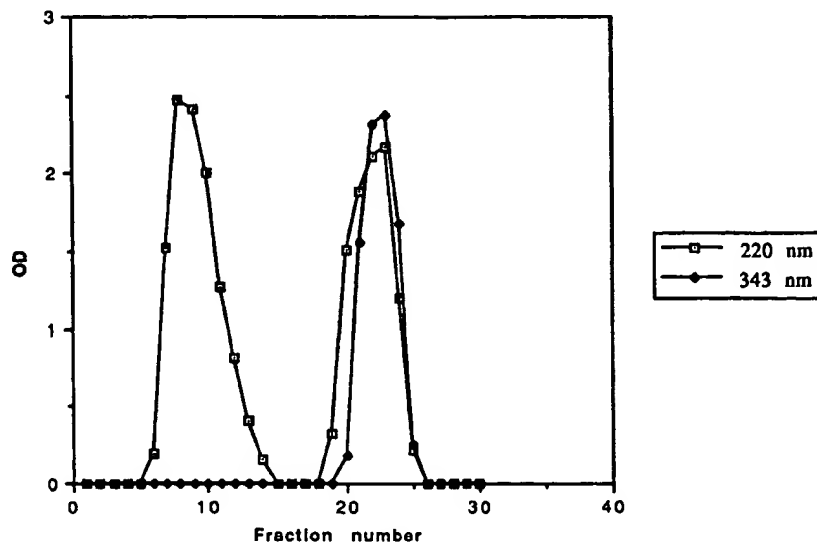
Release Studies. Release of the peptide FR₃C by reductive cleavage of its disulfide linkage to PEG-cyste-

amine was evaluated using 3 mM glutathione in PBS (pH 7.4) at room temperature. At each time point, an aliquot was withdrawn and acidified to halt the disulfide interchange reaction. Released peptide was removed from PEG—peptide conjugate by gel filtration chromatography, and the ratio of PEG (i.e., Lys residues) to peptide (i.e., Phe or Arg residues) was determined by amino acid analysis. Release was found to be relatively rapid, with a half-time of about 3 min (data not shown). The presence of glycine and glutamic acid in the high-molecular-weight fraction from glutathione-treated samples (data not shown) indicates that glutathione replaces the released peptide on the PEG copolymer.

Release kinetics were also studied using the disulfide-linked radiolabeled peptides, Tat9-Cys and Tat9K(bio)-Cys. Released peptide was removed from PEG—peptide conjugate by ultrafiltration. The half-time of release in PBS containing 3 mM glutathione was found to also be about 3 min for either peptide (Figure 3).

To achieve a slower release rate, as previously suggested for linking antibodies to toxins (*9*), the PEG derivative of the sterically hindered cysteamine analogue, 1-amino-2-methyl-2-propanethiol, was synthesized. Analysis of the release rate of radiolabeled Tat9K(bio)-Cys gave a half-time of about 40 min in the presence of 30 mM glutathione (Figure 4). Since the disulfide cleavage rate is proportional to glutathione concentration (10), the sterically hindered linker has a release rate about 100-times slower than does the cysteamine linker. Thus, the release rate can be readily controlled by selection of the linker between the PEG backbone and the appended peptide.

Cell Assay. The ability to achieve a biological effect was tested using the peptide Tat9K(bio)-Cys, which represents the TAR RNA-binding domain of the Tat protein encoded in the human immunodeficiency virus (HIV-1) genome. The rationale is that Tat protein interacts with TAR, which comprises the 5′-terminus of nascent transcripts, to potentiate transcription elongation, and that a Tat-binding domain peptide might interfere with this transactivation process (*8*). Indeed, the Cys(S-biotin) analogue of this peptide has been shown to inhibit viral replication in infected cells, thereby being a candidate therapeutic agent for AIDS (*8*). The ap-

Figure 2. Purification of the product from a reaction mixture of PEG-cysteamine-TP and the peptide FR₃C by gel filtration chromatography. Note the presence of the released 2-thiopyridone in the low-molecular-weight fractions according to absorbance at 343 nm.
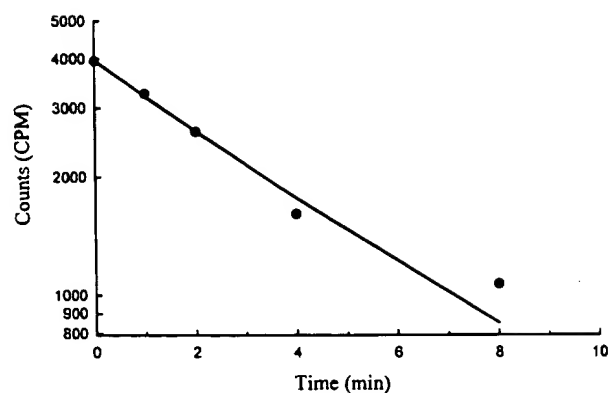
Figure 3. Time course of release of the radiolabeled peptide Tat9K(bio)-Cys from PEG-cysteamine-peptide by 3 mM glutathione in PBS. The data are presented as a semilog plot. Essentially the same release kinetics were obtained in two additional experiments.
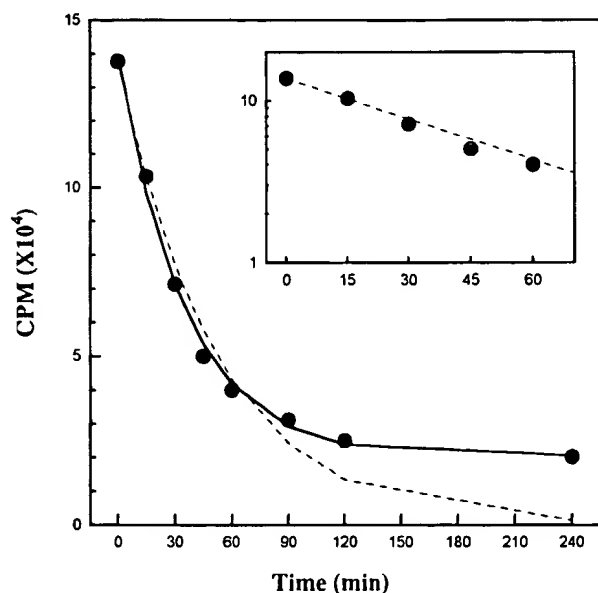

Figure 4. Time course of release of the radiolabeled peptide, Tat9K(bio)-Cys, from PEG-1-amino-2-methyl-2-propanethiol-peptide in PBS by 30 mM glutathione. The dashed line is a theoretical plot of $C = C_{initial}e^{-kt}$. A semilog plot of the early time point data is shown in the inset. Essentially the same release kinetics were obtained in two additional experiments.

pended biotin moiety has been found to increase cell uptake of the peptide (*8*). The Lys(ε-biotin) analogue of this peptide, used in the present study, has been found to bind to TAR RNA with similar avidity and specificity as the Cys(S-biotin) analogue and to inhibit gene expression (Figure 5) in a model cell assay (*8*), and it would be expected to inhibit HIV-1 replication similarly. A conjugate comprising multiple copies of this peptide disulfide-linked to PEG, PEG-[cysteamine-Tat9K(bio)-Cys]₈, was not only active in the model cell assay but also resulted in an increase in potency (Figure 5).

DISCUSSION

Although peptides and peptide mimetics are potential therapeutic agents, a major limitation to their utility is the requirement of parenteral rather than oral administration, due to degradation and/or poor absorption in the gastrointestinal tract. The necessity of frequent injections of a therapeutic peptide, due to the rapid
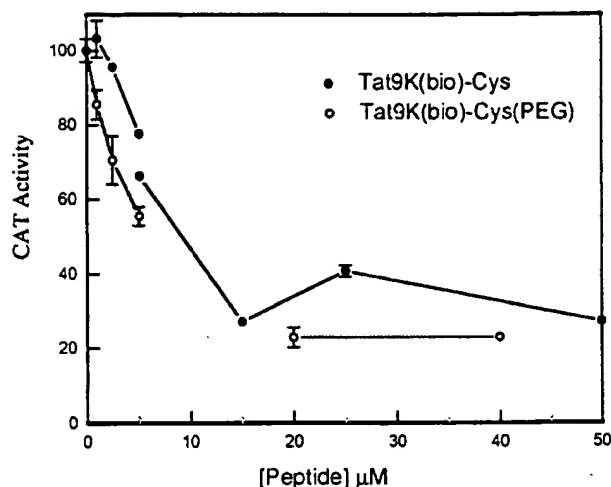
Figure 5. Inhibition of protein expression from a TAR-CAT plasmid. The biotinylated Tat-peptide inhibitor, either free or appended to the PEG carrier, was added at each indicated concentration. Each point is the average of three separate cell cultures. The data for the low concentrations of free and appended peptide were obtained in a side-by-side experiment, whereas the data for the high concentrations were obtained in separate experiments. Note the repetition of one concentration of free Tat-peptide in the high and low concentration sets of experiments; this is indicative of the assay-to-assay variability. The remaining 20—25% of CAT Activity at high inhibitor concentrations most likely represents CAT protein already synthesized prior to addition of the inhibitor to the culture medium and its uptake into the cells.

clearance of low-molecular-weight compounds, can be overcome by using PEG as a carrier (*4*). In this report, we describe an approach for preparing a reversible conjugate of a peptide on a PEG polymer. The reversible linkage is the disulfide bond, which can be cleaved by glutathione, a physiologically relevant reducing agent. This concept has recently been reported using hemoglobin as the carrier, with disulfide linkage to a cysteine residue in the peptide (10). In that study (10), mathematical modeling was presented to show the influence of various kinetic parameters on the blood level of released peptide.

In our studies, release of the peptide from the polymer was studied in PBS containing reduced glutathione, which is present in most tissues at a concentration of approximately 3 mM (*11*). Since the concentration of reduced glutathione in blood is on the order of 10 μM (*12*), the appended peptide molecules should remain mostly bound to the PEG carrier in the extracellular environment, but they should be released from the carrier upon entry into cells. Thus, this disulfide-based PEG delivery approach may be especially advantageous for intracellularly targeted drugs.

We now speculate that a PEG carrier loaded with multiple copies of the peptide, Tat9K(bio)-Cys (or a peptidase-resistant version), could be a particularly useful therapeutic product. Owing to its low clearance rate and resistance to disulfide exchange in extracellular fluids, this conjugate would be parenterally administered at, perhaps, daily or weekly intervals. The multiple biotin moieties appended to each PEG molecule, as well as the high density of positive charges on the side chains of the basic amino acids, might have an additive or synergistic effect on cell uptake efficiency. Indeed, preliminary cell culture experiments indicate that the peptide is more potent when added to the culture medium as a disulfide-linked PEG conjugate. Although we have not yet experimentally determined the basis for this apparent increase

in potency, we hypothesize that it is due to enhanced cellular uptake. Whatever the reason, it is clear that both an uptake enhancer (biotin) and a PEG carrier contribute markedly to enhanced potency for a peptide that has an intracellular target. In conclusion, our approach provides a method for reaching intracellular disease-related targets using peptide mimetics and other polar organic compounds that would otherwise not have the requisite pharmacologic properties.

ACKNOWLEDGMENT

LITERATURE CITED

(1) Duncan, R., and Kopacek, J. (1984) Soluble synthetic polymers as potential drug carriers. *Adv. Polym. Sci. 57*, 53−101.

(2) Zalipsky, S. (1995) Functionalized poly(ethylene glycol) for preparation of biologically relevant conjugates. *Bioconj. Chem. 6*, 150−165.

(3) Davis, S., Abuchowski, A., Park, Y. K., and Davis, F. F. (1981) Alteration of the circulating half-life and antigenic properties of bovine adenosine deaminase in mice by attachment of poly(ethylene glycol). *Clin. Exp. Immunol. 46*, 649−652.

(4) Nathan, A., Zalipsky, S., Ertel, S. I., Agathos, S. N., Yarmush, M. L., and Kohn, J. (1993) Copolymers of lysine and poly(ethylene glycol): A new family of functionalized drug carriers. *Bioconj. Chem. 4*, 54−62.

(5) Woghiren, C., Sharma, B., and Stein, S. (1993) Protected thiol-poly(ethylene glycol): A new activated polymer for reversible protein modification. *Bioconj. Chem. 4*, 314−318.

(6) Grassetti, D. R., and Murray. J. R. (1967) Determination of sulfhydryl groups with 2, 2′- or 4, 4′-dithiodipyridine. *Arch. Biochem. Biophys. 119*, 41−49.

(7) Riddles, P. W., Blakeley, R. L., and Zerner, B. (1979) Ellman's reagent: 5,5′-Dithiobis(2-nitrobenzoic acid)-a reexamination. *Anal. Biochem. 94*, 75−81.

(8) Choudhury, I., Wang, J., Rabson, A. B., Stein, S., Pooyan, S., Stein, S., and Leibowitz, M. J. (1998) Inhibition of HIV-1 replication by a Tat RNA-binding domain peptide analogue. *J. Acquired Immune Defic. Syndr. 17*, 104−111.

(9) Goff, D. A., and Carroll, S. F. (1990) Substituted 2-iminothiolanes: Reagents for the preparation of disulfide cross-linked conjugates with increased stability. *Bioconjugate Chem. 1*, 381−386.

(10) Trimble, S. P., Marquardt, D., and Anderson, D. C. (1997) Use of designed peptide linkers and recombinant hemoglobin mutants for drug delivery: In vitro release of an angiotensin II analogue and kinetic modeling of delivery. *Bioconj. Chem. 8*, 416−423.

(11) Meister, A., Griffith, O. W., and Tate, S. S. (1979) New aspects of glutathione metabolism and translocation in mammals. *Ciba Found. Symp. 72*, 135−161.

(12) Meister, A. (1991) Glutathione deficiency produced by inhibition of its synthesis and its reversal; applications in research and therapy. *Pharmacol. Ther. 51*, 155−194.

BC980038P

BBA

Riboflavin-mediated delivery of a macromolecule into cultured human cells

Susan R. Holladay, Zhen-fan Yang, Michael D. Kennedy, Christopher P. Leamon, Robert J. Lee, M. Jayamani, Thomas Mason, Philip S. Low *

Department of Chemistry, 1393 Brown Bldg., Purdue University, West Lafayette, IN 47907-1393, USA

Abstract

Cell surface receptors for the vitamins folic acid and biotin have been previously reported to mediate the endocytosis of vitamin-conjugated macromolecules into cultured cells. To evaluate whether a similar uptake pathway for riboflavin-conjugated macromolecules might exist, riboflavin was covalently linked to bovine serum albumin (BSA) via the vitamin's ribityl side chain, and uptake of the protein by cultured human cells was examined. Whereas unconjugated BSA was not internalized by KB, A549, SK-LU-1 or SK-OV cells, riboflavin-conjugated BSA was readily internalized ($> 10^6$ molecules/cell). Analysis of the uptake pathway revealed that the riboflavin-BSA conjugate likely docks on cells at a carrier/transport protein that is distinct from the uptake pathway for free riboflavin and then enters via normal membrane cycling. Evidence for this contention is: (i) the internalized conjugate accumulates in endosomal compartments, (ii) uptake into cells is halted at temperatures near 0°C where membrane trafficking is abrogated, (iii) cell association is inhibited by unlabeled riboflavin-BSA, but not by free riboflavin, and (iv) cellular uptake of [^{3}H]riboflavin is only partially inhibited by riboflavin-BSA. Regardless of the pathway of internalization, these data demonstrate that riboflavin conjugation can facilitate protein entry into human cells in culture. © 1999 Elsevier Science B.V. All rights reserved.

Keywords: Riboflavin transport; Receptor-mediated endocytosis; Drug delivery; Vitamin-mediated protein uptake

1. Introduction

Delivery of toxins, genes, chemotherapeutic agents, antisense oligonucleotides, and enzymes into cells for medicinal purposes has been limited by the low permeabilities of the aforementioned molecules through the cell's plasma membrane. As a conse-quence, significant effort has been devoted to identifying cell surface ligands that might be exploited to carry attached molecules into cells via the natural endocytosis pathways of their membrane bound receptors. Varying degrees of success have been achieved by this method with targeting ligands such as asialoglycoproteins [1], monoclonal antibodies [2], transferrin [3], epidermal growth factor [4], insulin [5], human chorionic gonadotropin [6], biotin [7], interleukin 6 [8], vitamin B-6 [9], and folic acid [10]. Importantly, where both cell specificity and uptake capacity of a cell surface ligand are high, numerous applications of the corresponding delivery technology are readily envisioned [2,3,5–9,11], suggesting

---

that if new targeting ligands can be identified, important uses may follow.

The observation that a common vitamin like biotin, vitamin B-6, or folic acid might be exploited for co-delivery of therapeutic drugs into target cells raises an obvious question: are other vitamins capable of a similar function? Recent research on the kinetics of riboflavin uptake across brush border membranes of the rat intestine suggests the involvement of two mechanisms [12,13]. First, using isolated liver cells [14] and renal cells [15], McCormick and colleagues have shown that riboflavin appears to enter cells via a saturable carrier-mediated pathway when the substrate concentration is near physiologic (a few μM). However, at substrate concentrations above 2 μM, riboflavin is thought to enter cells by unfacilitated diffusion. Studies on rabbit and human intestines confirm the participation of a carrier-mediated system [16,17], and research on cultured epithelial (Caco-2) cells indicates that most transport characteristics can also be reproduced in an experimentally approachable model system [18]. Nevertheless, although riboflavin-binding proteins have been found in various sources [19], no riboflavin carrier or membrane receptor has yet been isolated or identified.

Whether any of the possible riboflavin uptake routes can be exploited to co-deliver an exogenous unrelated molecule has never been addressed. However, cellular uptake of riboflavin-5′-α-D-glucoside, a naturally occurring adduct of riboflavin, has been documented [20], and riboflavin conjugation to serum albumin has been shown to facilitate the protein's movement across pulmonary epithelium [21]. As part of an ongoing effort to explore vitamin-mediated drug delivery pathways, we have undertaken to examine whether riboflavin might be capable of mediating uptake of otherwise impermeable molecules. For this purpose, we have covalently attached riboflavin to bovine serum albumin (BSA) at a site on riboflavin that does not compromise the vitamin's affinity for riboflavin binding proteins [13,16,22,23]. Because BSA (68 000 Da) is impermeable to cell membranes, this polypeptide constitutes a useful test molecule to evaluate the potential of a riboflavin-mediated transport pathway. We present evidence here that BSA-riboflavin likely enters cultured human cells via an endocytosis pathway and that this facilitated uptake occurs in quantities sufficient to justify further evaluation of the method for drug delivery applications.

2. Materials and methods

2.1. Materials

KB (human nasopharyngeal carcinoma), SK-LU-1 (human lung adenocarcinoma), SK-OV (human ovary adenocarcinoma), and A549 (human lung carcinoma) cells were obtained from the American Type Culture Collection or received as a gift from the Purdue Cancer Center (West Lafayette, IN). Tissue culture products were purchased from Gibco BRL. All other chemicals were reagent grade and obtained from major suppliers.

2.2. Cell culture

KB, SK-LU, SK-OV, and A549 cells were grown continuously as a monolayer using riboflavin-free Dulbecco's Modified Eagle's medium (RFDMEM) supplemented with penicillin (50 units/ml), streptomycin (50 μg/ml), L-glutamine (2 mM), amphotericin B (250 μg/ml), sodium pyruvate (100 mM) and 10% heat-inactivated fetal calf serum in a 5% CO_2/95% air humidified atmosphere at 37°C. The fetal calf serum contains sufficient riboflavin to sustain rapid cell growth indefinitely.

2.3. Conjugation of riboflavin to proteins

Dry riboflavin (200 mg) was dissolved in pyridine (320 μl) with ice cooling and treated with thionyl chloride (320 μl). The solution was then heated at 65°C for 16 h. Dimethylformamide (1 ml) was added to uniformly solubilize all components and 140 μl of the resulting solution containing activated riboflavin was added to BSA (20 mg) dissolved in 1 ml phosphate buffered saline (PBS) (Fig. 1). 1 M NaOH was added dropwise until the solution pH reached 8. The reaction was then allowed to proceed for 3 h at 23°C in the dark and the solution was centrifuged at $7000 \times g$ for 15 min to remove any particulates. The product in the supernatant was separated from the starting materials using a Sephadex G-25 column

equilibrated in PBS. The number of riboflavins conjugated to each protein was determined spectrophotometrically to be 5 ± 1 (see below). The integrity of the isoalloxazine ring system of the product was confirmed spectrophotometrically by comparison of its spectrum with unmodified riboflavin. BSA-riboflavin was found to be stable when stored at 4°C in the dark.

2.4. Quantitation of riboflavin bound per protein molecule

The extent of riboflavin conjugation to BSA was determined spectrophotometrically from the difference in absorption of BSA-riboflavin and unmodified BSA at 445 nm using the extinction coefficient at this wavelength of $\varepsilon = 4409$. The concentration of protein was evaluated using the BCA protein assay (Pierce). Many BSA-riboflavin preparations were used in this study, and for uniformity all of the data presented were collected with samples containing 5 ± 1 riboflavins per BSA. Higher label ratios increased non-specific binding and significantly lower ratios resulted in less efficient uptake (data not shown).

2.5. Labeling of BSA with fluorescein and rhodamine B

Bovine serum albumin conjugated to riboflavin or unconjugated BSA was dissolved in a minimal volume of PBS and incubated with a 20-fold molar excess of fluorescein isothiocyanate (FITC) for 3–4 h in the dark at 23°C. The labeled protein was separated from unreacted FITC using a 10 cm × 1 cm Sephadex G-25 column (Bio-Rad) equilibrated in PBS. The eluted fractions were collected, sterile filtered, and stored in the dark at 4°C.

BSA-riboflavin in PBS, pH 7.4, was also labeled with rhodamine B by incubating the conjugate for 2 h at room temperature in the dark with a 7-fold molar excess of lissamine rhodamine B sulfonyl chloride. Following derivatization, rhodamine B-BSA-riboflavin was separated from free fluorophore by Sephadex G-25 gel filtration chromatography.

2.6. ^{125}I Labeling of protein

BSA conjugated to riboflavin or unconjugated

BSA was dissolved in a minimal amount of NaH_2PO_4 buffer (0.1 M, pH 7.0). Pre-washed Iodo-Beads (Pierce) were incubated with $Na^{125}I$ (Amersham) for 5 min. The protein solution was then added to the $Na^{125}I$ Iodo-Bead mixture and the suspension was incubated at 23°C for 15–20 min. The labeled protein was separated from unreacted $Na^{125}I$ using a 10 cm × 1 cm Sephadex G-25 column equilibrated in PBS. The eluted fractions were collected, sterile filtered, and stored in the dark at 4°C.

2.7. Cellular uptake of fluorescent riboflavin-protein conjugates

KB, SK-LU, SK-OV, or A549 cells were initially grown for 2 days to near confluence in 60×10 mm Falcon culture dishes, after which the incubation medium was replaced with fresh RFDMEM. BSA labeled with both riboflavin and FITC, or BSA labeled with FITC alone (negative control) was then added to the dishes to a final concentration of 1.47 μM. The cells were incubated for 2 h in a humidified atmosphere at 37°C. The monolayers were rinsed 3 times with ice-cold PBS and the cells were then dissolved overnight in a 1% Triton X solution. Cell-associated FITC-BSA was quantitated by fluorescence using a Perkin Elmer MPF 44A fluorimeter ($\lambda_{ex} = 495$ nm, $\lambda_{eM} = 520$) and cellular protein was estimated using the BCA protein assay. Data are reported as the number of fluorescent BSA-riboflavin macromolecules per cell, based on experimentally determined conversion factors for the amount of protein per cell type (unpublished observations).

2.8. Cellular uptake of iodinated riboflavin-protein conjugates

KB cells were grown for 2 days in 35×10 mm Falcon culture dishes as described above, after which the incubation medium was replaced with fresh RFDMEM. For competition studies, unlabeled BSA-riboflavin was added to the cells 60 min prior to addition of labeled protein. ^{125}I-BSA-riboflavin or ^{125}I-BSA was then added to the desired dishes to the final concentrations indicated. The cells were incubated for 2 h in a humidified atmosphere at 37°C.
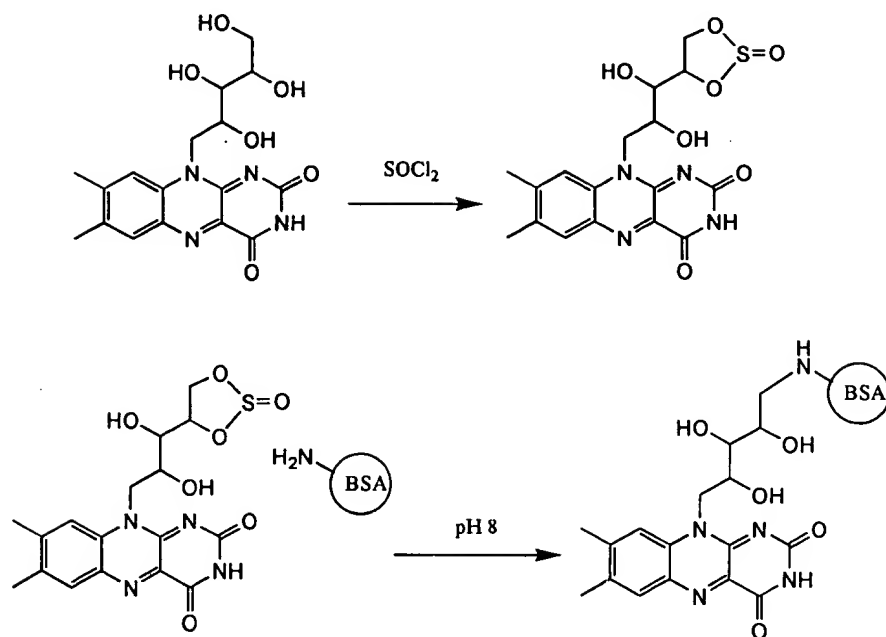
Fig. 1. Synthesis scheme of BSA-riboflavin. Although this diagram shows labeling only on the preferred 5' carbon of riboflavin, attachment to BSA could conceivably occur on any of the carbons of the ribityl group.

The monolayers were rinsed 3 times with ice-cold PBS and dislodged from the culture dish by scraping in cold PBS. The cells were centrifuged at $1000 \times g$ for 1 min, the supernatant was replaced with ice-cold PBS, and the pellet was resuspended and pelleted 3 times. The pelleted cells were then dissolved overnight in a 3:10 solution of 1 M NaOH and BCA reagent 'A' (BCA protein assay, Pierce). Samples were counted for ^{125}I-BSA-riboflavin in a Packard Cobra γ-counter, and total cellular protein was determined using a BCA protein assay kit (Pierce).

2.9. Confocal microscopy

KB cells were grown and treated as described above, except all fluorescent protein samples were added at a final protein concentration of 0.44 μM. Cells were washed as described in previous experiments and mounted on glass slides. Cell-associated fluorescence was then imaged with a Bio-Rad MRC/500 confocal laser scanning microscope using a 488 nm excitation wavelength. For the images displayed in this report, the focal plane was as near the center of the cell as possible.

3. Results

Although the riboflavin transport data reported to date suggest the involvement of some type of plasma membrane carrier [14], the data do not necessarily exclude the possible participation of a receptor that could deliver riboflavin conjugates into a cell by endocytosis. Since receptor-mediated uptake pathways for folate, vitamin B-6, and biotin have been readily distinguished from carrier-mediated pathways by their abilities to co-internalize attached macromolecules [7,9,10], we looked to see whether some cells might also be able to internalize riboflavin-macromolecule conjugates. For this purpose, riboflavin was covalently linked to BSA, a protein of 68 000 Da, via a site on the ribityl side chain not believed to be involved in transporter recognition (Fig. 1) [13,16,22,23]. Cells were then treated with the riboflavin-conjugated BSA in the presence or absence of competitive ligands and cellular uptake was monitored. To visually observe whether rhodamine-BSA-riboflavin actually enters the cell interior, confocal fluorescence microscopy was employed to monitor entry of the conjugate into cultured KB cells, a human nasopharyngeal cancer cell line. In all cases, the
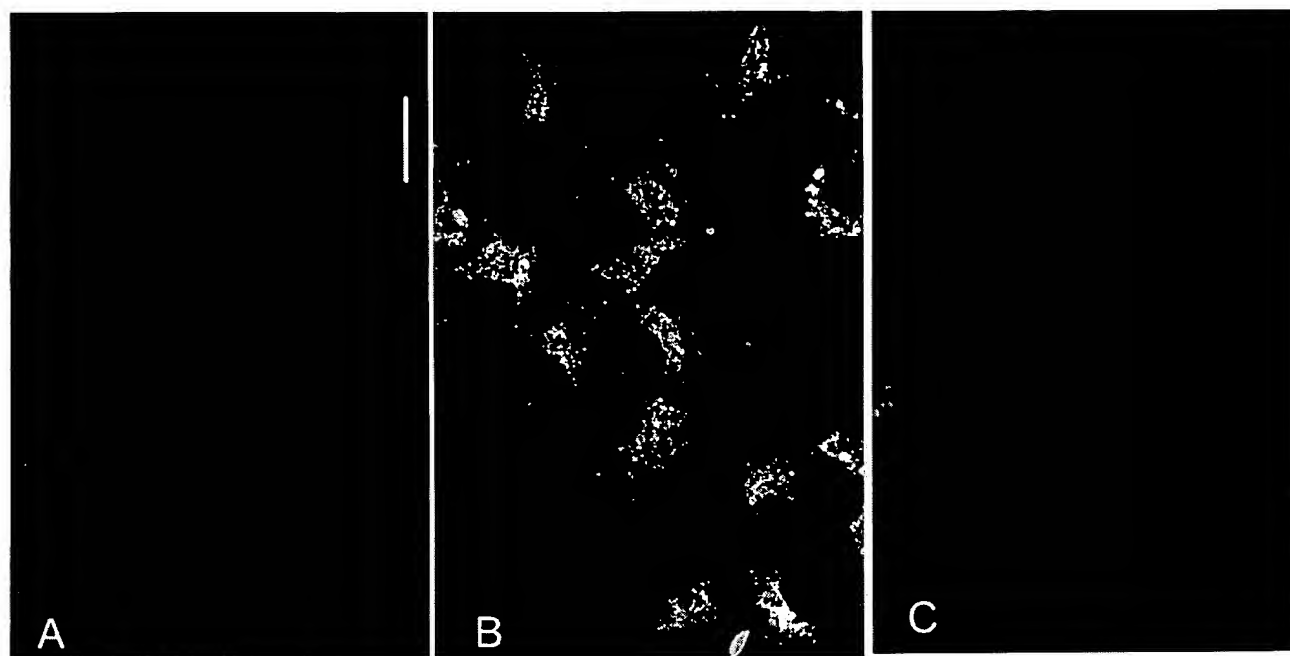
Fig. 2. Confocal microscopy of the distribution of rhodamine-BSA-riboflavin at a central horizontal plane within KB cells. KB cells were incubated for 2 h at 37°C with (A) unsupplemented growth medium (control), (B) 0.44 µM rhodamine-BSA-riboflavin, or (C) 0.44 µM rhodamine-BSA. After rinsing 3× in cold PBS, the cells were transferred to a glass slide and viewed by confocal microscopy using optics set for rhodamine observation.

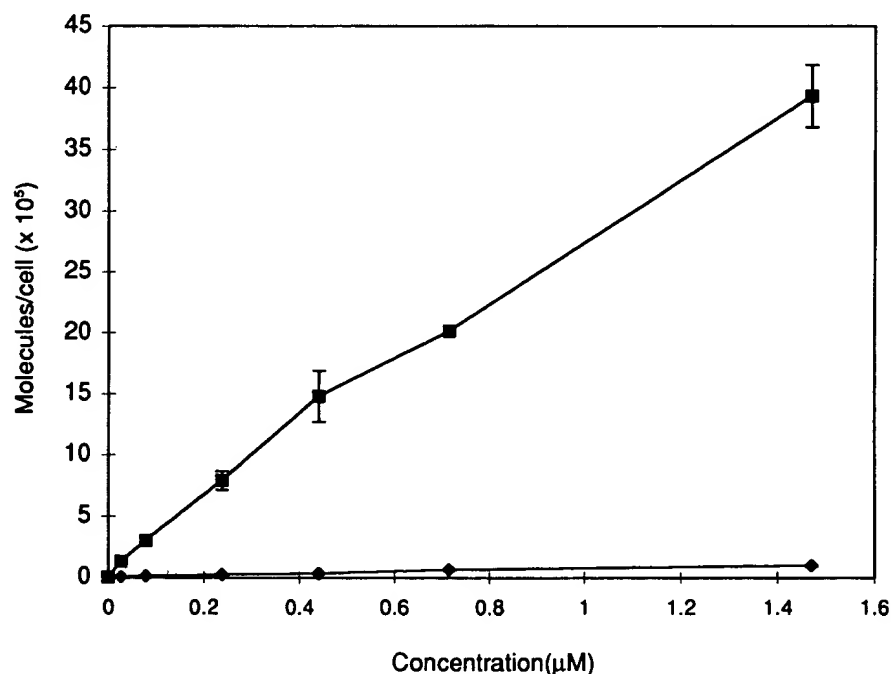Fig. 3. Concentration-dependent association of ^{125}I-BSA-riboflavin with KB cells. KB cells were incubated for 2 h at 37°C with the indicated concentrations of ^{125}I-BSA-riboflavin (■) or ^{125}I-BSA (♦), and then thoroughly washed and counted for radioactivity, as described in Section 2. Each point represents the mean of three trials, and error bars correspond to 1 S.D. In some cases the error bars lie within the dimensions of the data point.
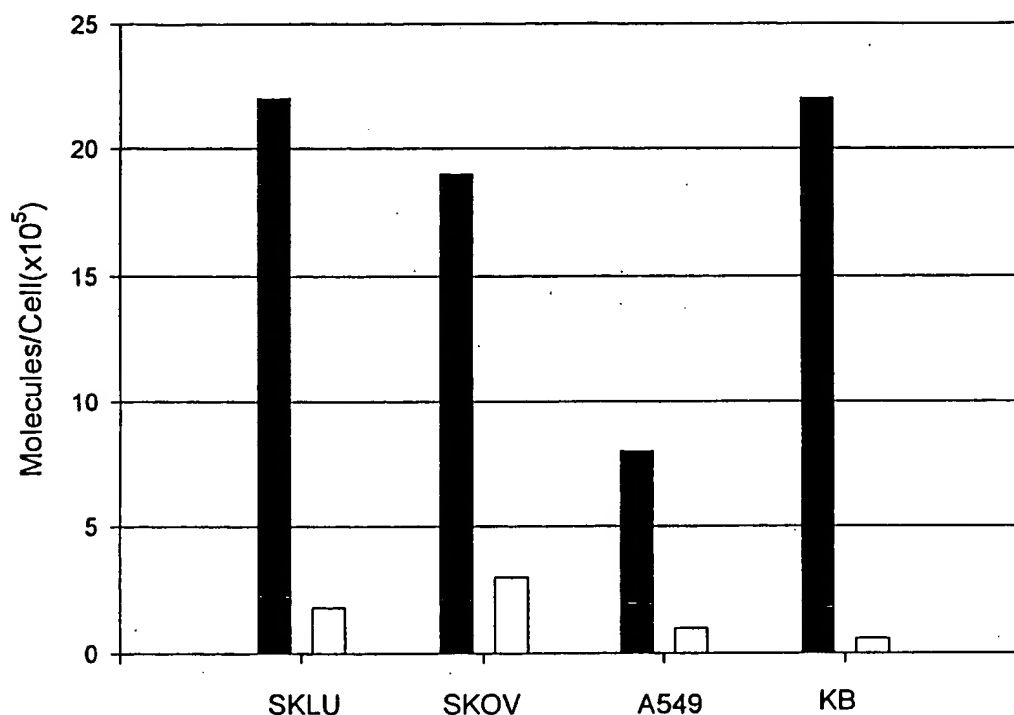
Fig. 4. Uptake of FITC-BSA-riboflavin by various human cell lines. The indicated cells were grown to near confluence in 60×10 mm Falcon culture dishes and then incubated for 2 h at 37°C in fresh RFDMEM containing either FITC-BSA-riboflavin (solid bars) or FITC-BSA (open bars). After washing, cell-associated fluorescein fluorescence was quantitated by dissolving the cells in detergent and measuring their fluorescence in a Perkin Elmer MPF-44A fluorimeter (λ_{ex} = 495 nm, λ_{em} = 520 nm).

plane of data collection was set near the center of the cell to allow evaluation of conjugate internalization independent of cell surface binding. Micrograph A shows the absence of measurable autofluorescence of KB cells treated with no fluorescent BSA. In contrast, cells incubated for 2 h at 37°C with 0.44 µM rhodamine-BSA-riboflavin exhibit a punctate distribution of fluorescence over the entire cell interior, with a lower frequency of intensities in the nuclear region of the cell (panel B). Such a staining pattern is reminiscent of endocytic vesicles, which are often abundant in the cytoplasm but generally less concentrated where the nucleus dominates the intracellular space. Importantly, cells treated identically with rhodamine-BSA (no riboflavin) display negligible internalized fluorescence (panel C), suggesting uptake of the fluorescent BSA-riboflavin is strongly riboflavin dependent.

To obtain a more quantitative evaluation of the capacity of riboflavin to mediate BSA uptake, BSA was radio-iodinated and endocytosis of its riboflavin conjugate was determined by γ-counting under essen-

tially the same incubation conditions employed in Fig. 2. As shown in Fig. 3, ^{125}I-BSA-riboflavin association with KB cells is strongly concentration dependent, increasing nearly linearly with the level of conjugate in the medium. By 1.5 µM concentration, where the response is still linear, roughly 4×10^6 riboflavin conjugates are bound or internalized per cell, suggesting the capacity of the pathway at saturation should be even higher. In an analogous study conducted with FITC-BSA-riboflavin, concentrations extending to 4.4 µM were examined and still no indication of saturation was observed (data not shown). Importantly, ^{125}I-BSA (diamond symbols) displays no tendency to associate with the KB cells, confirming that the BSA uptake must be riboflavin mediated. This conclusion was confirmed by studies with several other proteins (data not shown[1]) that revealed similar riboflavin-dependent uptake.

---

[1] During the course of the studies of BSA-riboflavin uptake, we have examined the internalization of IgG, ferritin, and ribonuclease conjugates of riboflavin and obtained qualitatively similar results.
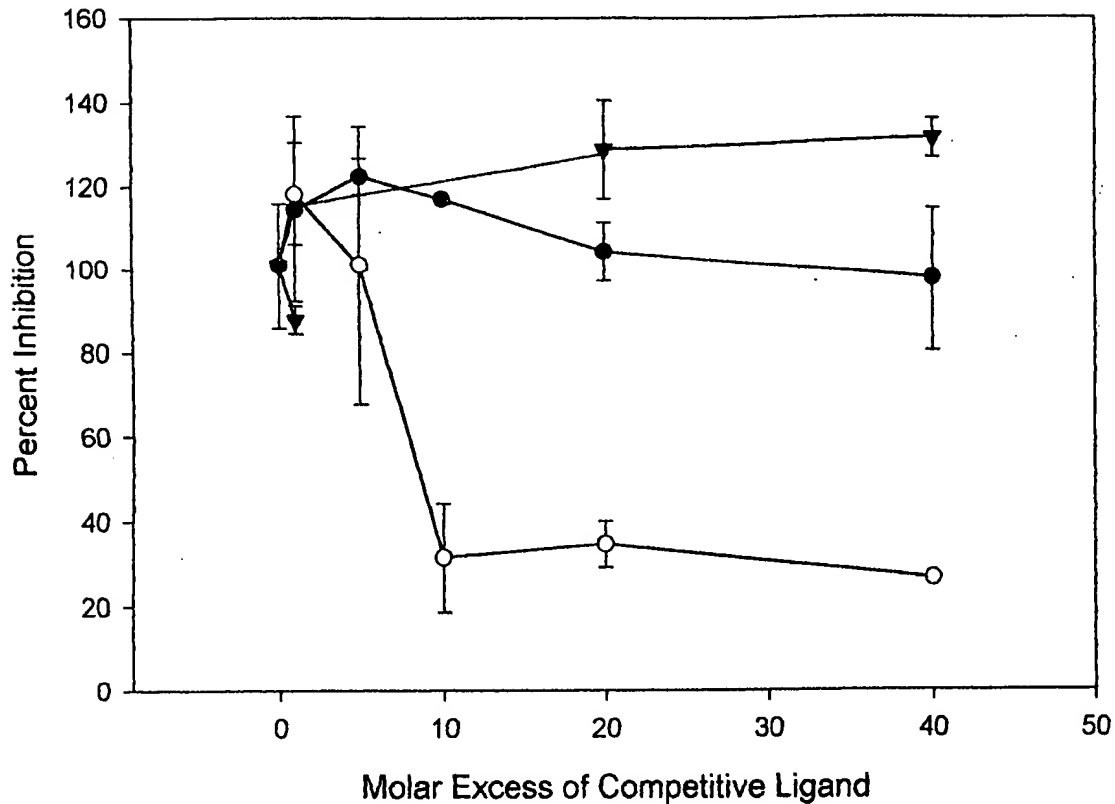
Fig. 5. Competitive inhibition of BSA-riboflavin uptake by KB cells using riboflavin, riboflavin-5′-phosphate, or unlabeled BSA-ribo-flavin as the competitive ligand. KB cells were grown to near confluence in RFDMEM and treated for 1 h at 37°C with the indicated concentrations of competitive ligand: BSA-riboflavin (○); riboflavin (●), and FMN (▼). ^{125}I-BSA-riboflavin (0.075 μM) was then added and allowed to incubate for 2 h at 37°C. After washing, cell uptake of the labeled BSA-riboflavin was quantitated as described in Section 2.

In order to show that the internalization process is not specific to KB cells, FITC-BSA-riboflavin uptake was studied in three other cell lines grown for several weeks in riboflavin-deficient medium: SK-LU-1, SK-OV, and A549 cells. As shown in Fig. 4, each of the cell lines can take up the riboflavin conjugates, albeit with different capacities. Further, cell association is invariably strongly riboflavin dependent, as shown by comparison of the solid versus open bars. Because KB cells exhibit the highest uptake capacity with the lowest non-specific binding of vitamin-free BSA, this cell line was selected for the remaining studies.

To further characterize the riboflavin-mediated BSA uptake pathway, the ability of free riboflavin or flavin mononucleotide (FMN) to competitively inhibit BSA-riboflavin uptake was examined. Curiously, even at a 40-fold molar excess of riboflavin or FMN, no diminution in binding of the macromo-lecular conjugate was observed (Fig. 5). In contrast, unlabeled BSA-riboflavin was found to dramatically reduce the uptake of its ^{125}I-labeled counterpart (Fig. 5). In view of the absence of any affinity of free ^{125}I-BSA for these KB cells (Fig. 3), competition for BSA binding sites cannot be responsible for this behavior. Instead, the data argue that a riboflavin-dependent binding site exists for riboflavin conjugates and that this site is not shared by the free vitamin or its phos-phorylated derivative (FMN). Importantly, the same lack of competition with riboflavin was also reported for the binding of riboflavin-5′-α-D-glucoside [20].

The apparent existence of a cell surface binding site with unique specificity for BSA-riboflavin was not anticipated. Indeed, analogous studies with BSA-folate and BSA-biotin had previously shown aggressive competition from the corresponding free vitamin [7,10], i.e. consistent with the existence of a
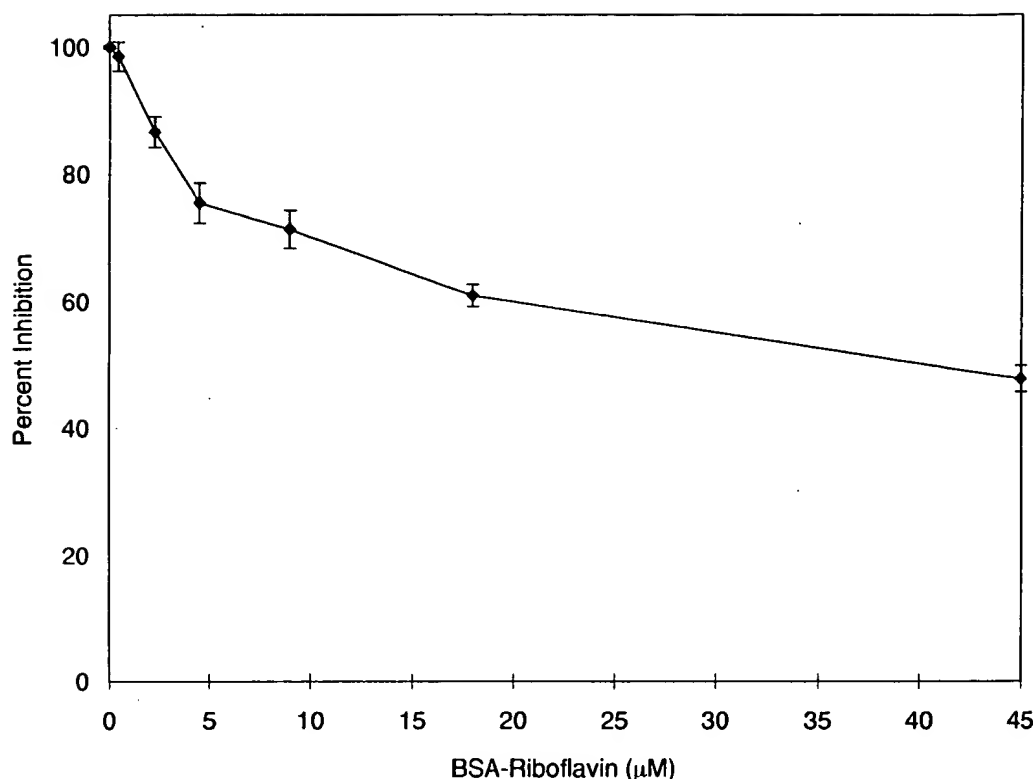
Fig. 6. Inhibition of [³H]riboflavin uptake into KB cells by increasing concentrations of BSA-riboflavin. KB cells were grown to near confluence in RFDMEM in 35×10 mm Falcon culture dishes. Directly prior to each experiment, the medium was replaced with fresh RFDMEM, and the cells were then treated for 1 h with the indicated concentrations of BSA-riboflavin. [³H]Riboflavin (0.45 μM) was then added to the culture dishes and riboflavin transport was allowed to proceed for 2 h. Cells were then washed and counted for radioactivity, as described in Section 2. Each data point represents the average of three trials ±S.D.

cell surface vitamin receptor. The absence of competition in the case of riboflavin and its conjugates would therefore seem to require a distinct mechanism of conjugate recognition and endocytosis. One possibility is that the normal uptake pathway of free riboflavin involves a transporter which can bind riboflavin conjugates. Because the conjugates would be too large to pass through the carrier's channel, they would only enter the cell during the normal course of membrane recycling. In contrast, natural substrates of the carrier protein such as riboflavin would rapidly move into the cell, thereby losing the ability to competitively block riboflavin conjugate binding. Although a thorough test of this hypothesis is beyond the scope of this investigation, we felt it would be instructive to simply examine whether BSA-riboflavin conjugates might alter the uptake of riboflavin at its natural carrier or transport site. For this purpose, [³H]riboflavin uptake was measured as a function of the concentration of BSA-riboflavin. As seen in Fig. 6, addition of BSA-riboflavin inhibited uptake of the free vitamin, but only at high concentrations of BSA-riboflavin. By 18 μM BSA conjugate, riboflavin transport was reduced to approx. 60% of the control value, suggesting that riboflavin and its BSA conjugate interact with the cells at a similar site. Whether BSA-riboflavin enters cells primarily as a complex with this carrier cannot be ascertained from the data.

Finally, to explore whether eventual BSA-riboflavin internalization might derive from some form of membrane trafficking, uptake of the conjugate was compared at 0, 25, and 37°C, where membrane cycling is halted, significantly retarded, or unabated, respectively [24,25]. Importantly, BSA-riboflavin uptake reached 1.6×10^6 molecules/KB cell at 37°C under the assay conditions employed. However, this number of cell-associated conjugates rapidly dimin-

ished to <20% of this value (3×10^5 molecules/cell) upon lowering the temperature to 25°C, and by 0°C, where membrane flow is completely abrogated, cell association was only 7.5% of normal (1.2×10^5 molecules/cell). Presumably, this latter value reflects the population of surface bound conjugates that are membrane-bound, but not yet internalized due to the blockade in membrane cycling. While these results are not inconsistent with an internalization mechanism based on some type of bilayer permeation, they are more strongly supportive of an uptake pathway involving membrane trafficking.

4. Discussion

We have shown that BSA can be delivered into intracellular compartments of several cultured human cell lines if the protein is first attached to riboflavin on the ribityl chain. Deletion of the vitamin was found to eliminate cellular uptake, and replacement of ^{125}I for FITC, or ribonuclease/ferritin/IgG for BSA exerted no effect on delivery, suggesting the moiety responsible for uptake is indeed the riboflavin. While competition studies revealed a complexity in the delivery pathway not readily explained by classical receptor-mediated endocytosis, the size of the BSA molecule and the strong suppression of internalization at temperatures below physiological values suggest the uptake still occurs by endocytosis/pinocytosis rather than facilitated diffusion across the plasma membrane. Indeed, the clear visualization of localized intensities of internalized conjugate inside the cell suggests an endosomal localization of the delivered polypeptide. One hypothesis consistent with all of the data is that riboflavin conjugates bind to a riboflavin transporter and enter cells via passive membrane cycling. In this scenario, free riboflavin would not compete well with BSA-riboflavin, because the unligated vitamin would rapidly pass on through the transporter. BSA-riboflavin, in contrast, would compete with free [^{3}H]riboflavin, because the vitamin conjugate would remain associated with the transport site. Based on both the direct binding (Fig. 3) and competitive binding (Fig. 6) studies, the affinity of BSA-riboflavin for its membrane site must be in the micromolar range.

Because similar studies have been conducted using folate as the targeting vitamin, some comparison of the two pathways might be instructive. While both vitamins can facilitate internalization of a variety of proteins, the affinities of the two systems for their vitamins differ greatly. Whereas the folate receptor binds folate conjugates with a K_d near 10^{-9} M [10,26], the riboflavin docking site associates with riboflavin conjugates with at best micromolar affinity. Consequently, to deliver a comparable number of macromolecules into a cell, it would be necessary to use considerably more riboflavin conjugate than folate conjugate under subsaturating conditions. Another significant difference is that while folate macromolecule uptake can be inhibited with free folate [10], free riboflavin does not obstruct riboflavin macromolecule internalization. Further, while mildly acidic washes efficiently remove folate-linked macromolecules that have not been internalized, these washes do not strip significant amounts of bound riboflavin macromolecule conjugates from the same cell surfaces (data not shown). Finally, while the folate receptor is predominantly expressed on cancer cells [27], our preliminary studies have shown a measurable uptake rate of riboflavin conjugates in some normal cells. Clearly, the two vitamin-mediated delivery pathways have very different properties. It will be interesting to evaluate which tissues are most active in internalizing riboflavin conjugates and to learn whether the uptake system might be exploited for tissue-selective drug targeting in vivo.

Acknowledgements

References

[1] G.Y. Wu, C.H. Wu, J. Biol. Chem. 262 (1987) 4429–4432.
[2] S. Olsnes, K. Sandvig, P.L. Peterson, P.I.v. Deurs, Immunol. Today 10 (1989) 291–295.
[3] E. Wagner, M. Zenke, M. Cotton, H. Beug, M.L. Birnsteil, Proc. Natl. Acad. Sci. USA 87 (1990) 3410–3414.
[4] D.L. Simpson, D.B. Cawley, H.R. Herschman, Cell 29 (1982) 469–473.
[5] M.J. Poznansky, K. Hutchinson, P.J. Davis, FASEB J. 3 (1989) 152–156.

[6] T.N. Oelfmann, E.C. Heath, J. Biol. Chem. 254 (1979) 1028–1032.

[7] M.A. Horn, P.F. Heinstein, P.S. Low, Plant Physiol. 93 (1990) 1492–1496.

[8] C.B. Siegall, D.J. Fitzgerald, I. Pastan, J. Biol. Chem. 265 (1990) 16318–16323.

[9] Z. Zhang, D.B. McCormick, Proc. Natl. Acad. Sci. USA 88 (1991) 10407–10410.

[10] C.P. Leamon, P.S. Low, Proc. Natl. Acad. Sci. USA 88 (1991) 5572–5576.

[11] C.P. Leamon, P.S. Low, J. Biochem. 291 (1993) 855–860.

[12] S. Feder, H. Daniel, G. Rehner, J. Nutr. 121 (1991) 72–79.

[13] D. Casirola, G. Gastaldi, G. Ferrari, S. Kasai, G. Rindi, J. Membr. Biol. 135 (1993) 217–223.

[14] T.Y. Aw, D.P. Jones, D.B. McCormick, J. Nutr. 113 (1983) 1249–1254.

[15] D.M. Bowers-Komro, D.B. McCormick, in: D.E. Edmondson, D.B. McCormick (Eds.), Walter Gruyter and Co., Berlin, 1987.

[16] H.M. Said, R. Mohammadkhani, E. McCloud, Proc. Soc. Exp. Biol. 202 (1993) 428–434.

[17] H.M. Said, P. Arianias, Gastroenterology 100 (1991) 82–88.

[18] H.M. Said, T.Y. Ma, Am. J. Physiol. 266 (1994) G15–G21.

[19] H.B. White, A.H. Merrill Jr., Annu. Rev. Nutr. 8 (1988) 279–299.

[20] T. Joseph, D.B. McCormick, J. Nutr. 125 (1995) 2194–2198.

[21] O.D. Wangensteen, M.M. Bartlett, J.K. James, Z.F. Yang, P.S. Low, Pharm. Res. 13 (1996) 1861–1864.

[22] D. Casirola, S. Kasai, G. Gastaldi, G. Ferrari, K. Matsui, J. Nutr. Sci. 40 (1994) 289–301.

[23] H.M. Said, D. Hollander, R. Mohammdkhani, Biochim. Biophys. Acta 1148 (1993) 263–268.

[24] R.G.Q. Leslie, Eur. J. Immunol. 10 (1980) 323–333.

[25] G. Carpenter, S. Cohen, J. Cell Biol. 71 (1976) 159–171.

[26] B.A. Kamen, A. Capdevila, Proc. Natl. Acad. Sci. USA 83 (1986) 5983–5987.

[27] S.D. Weitman, R.H. Lark, L.R. Coney, D.W. Fort, V. Frasca, V.R. Zurawski, B.A. Kamen, Cancer Res. 52 (1992) 3396–3401.